DAA/Langley

P-53

(NASA-CR-176202) FLOW ENERGIZERS. TASK A Progress Report (Texas A&M Univ.) 53 p Avail: NTIS HC AC4/MF A01 CSCL 01A

N87-28523

Unclas
G3/02 0097827

Date for general release August 1987

TEXAS ENGINEERING EXPERIMENT STATION
The Texas A&M University System
COLLEGE STATION, TEXAS 77843

TASK A

Flow Energizers

Progress Report

by

D. Ward and R. Binford
E. von Lavante and B. Paul

Aerospaced Engineering Department
Texas A&M University
College Station, TX 77843

Submitted to Langley Research Center
Hampton, Virginia
Technical Monitor: J. Stickle
Grant No.: NAG 1-344

TASK A: FLOW ENERGIZERS

Experimental

The primary objective during this reporting period was to collect pressure data and to develop the techniques and software for verifying the experimental results. Since the last written progress report, wing glove surface pressures have been measured in flight for two different energizer configurations, both with the left propeller feathered and with it running. Upper and lower surface pressure coefficients on the wing glove at an indicated airspeed of 85 knots are shown in Figure 1. With the exception of the point at 60% chord on the row of ports near the nacelle, the flight test data are consistent. As anticipated from the wind tunnel data, there is little change in pressure coefficient with and without the flow energizers. Immediately adjacent to the fuselage there does appear to be some increase in pressure coefficient due to the presence of the energizer. Also shown in Figure 1 are data from the wind tunnel for this flow energizer at the same angle of attack. With the exception of the nacelle pressure ports and considerably more scatter in the wind tunnel measurements, the two sets of data compare reasonably well.

Data reduction has been slower than anticipated, primarily because of difficulties in calibrating the seven-hole probes and in verifying the software. The first set of calibrations for the wake probe was incomplete and left some doubt as to the accuracy of the coefficients determined. A second calibration has now been run in the Texas A&M Low Speed Wind Tunnel and the data is now being processed to produce the calibration constants for these probes.

The data collected from the wake probe survey has been partially reduced, but the incomplete calibration constants and software glitches continue to plague the data reduction. The first information reduced is illustrated in Figure 2 and shows the velocity components at two different locations immediately behind the trailing edge at two different rake positions. The most interesting thing about this preliminary data is that there appears to be a reversal in sign of the v component of velocity near the fuselage with the propeller turning and with it feathered. Unfortunately, the data are for an energizer configuration that was installed in error. Nonetheless, this plot illustrates the kind of measurements that can be taken with the multi-hole wake rake probe. The next step is to carefully survey the area near the fuselage to see if the core of the vortex system can be located by looking at the velocity components in this plane. A series of flights will be flown shortly with their primary goal to collect this information.

The calibration, installation, and ground checkout of the strain gage balance to measure forces and moments on the flow energizer on the right sideof the fuselage of the test airplane

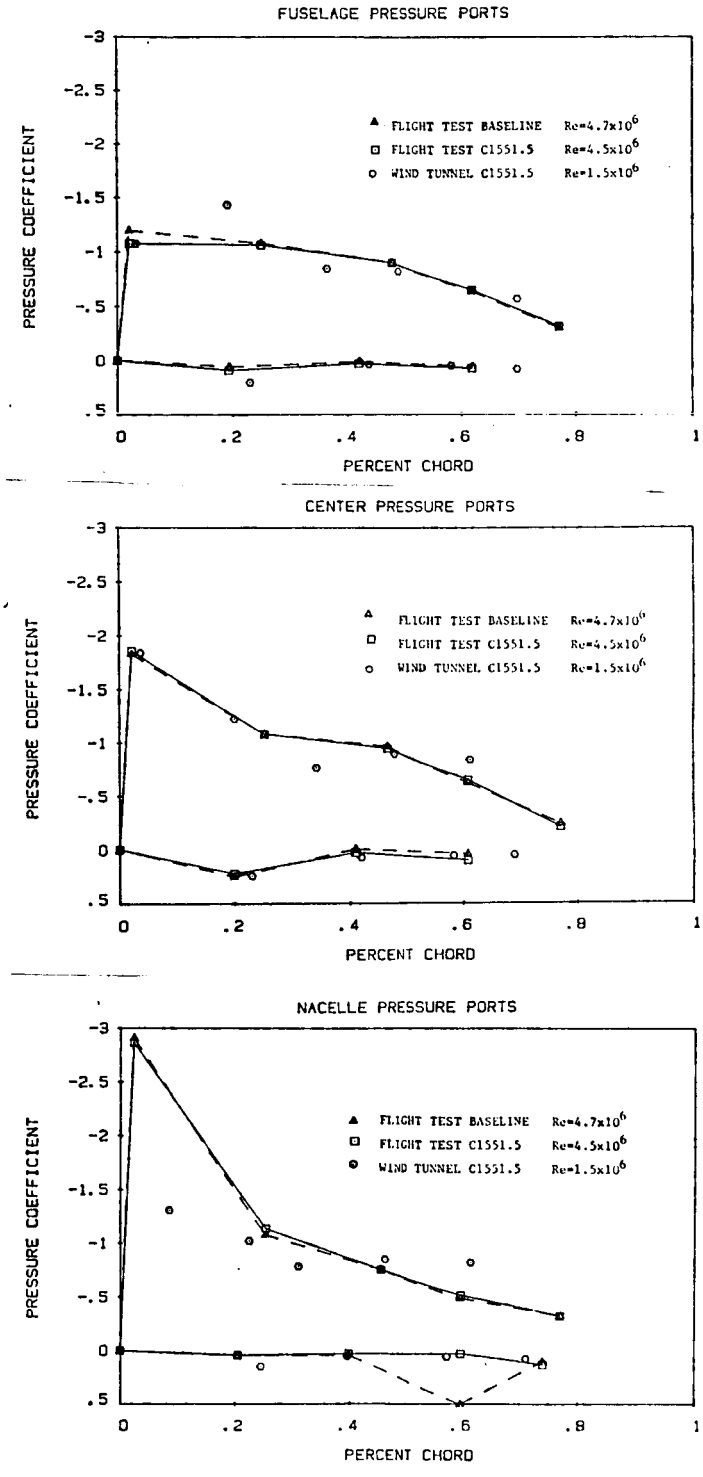

Figure 1. Glove Surface Pressure Coefficients (Airplane Angle of Attack: 8°)

is still behind schedule because of the data reduction workload. An undergraduate research assistant has been added to the team

for this summer to help speed up the data reduction and the installation of the strain gage balance. The first flight with the strain gage balance installed has now slipped to July 20 and meeting even that date is questionable.

The paper based on the wind tunnel tests of the 14 flow energizerconfigurations was published in the June 1985 issue of Journal of Aircraft.

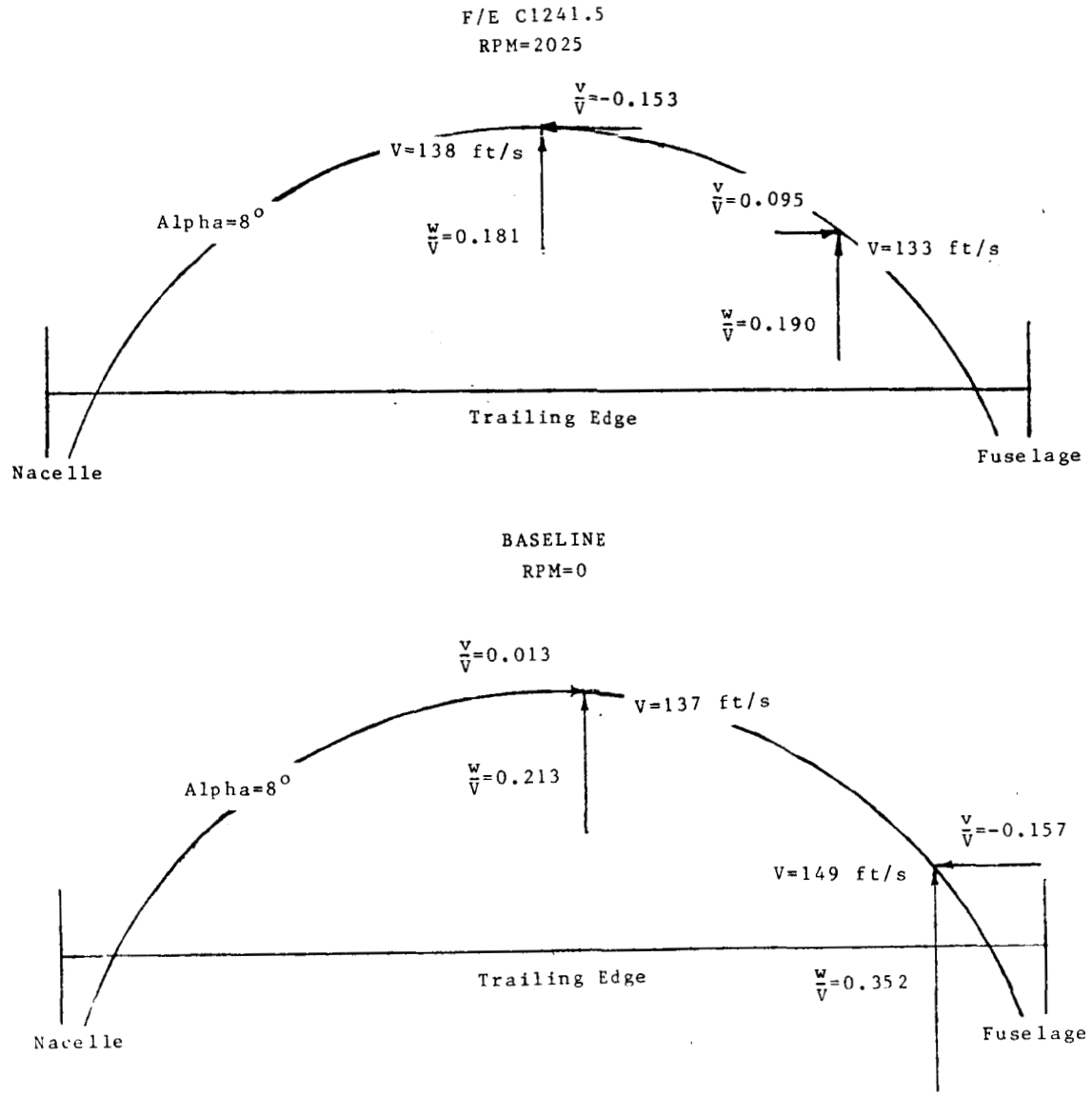

Figure 2. Wake Velocity Measurements
(Airplane Angle of Attack: 8°)

In summary, the experimental work is progressing and data have been collected. The results from the wind tunnel phase of the program have been presented at a national conference and are now available to designers through the Journal of Aircraft. Data reduction software continues to require considerable effort and has slowed installation of the strain gage balance for measuring forces and moments on the flow energizer. Some of the schedule slippage has been recovered since the last progress report, but the project is still behind schedule.

TASK A: FLOW ENERGIZERS

Numerical Part

The numerical part of Task A during the present reporting period can be divided into three parts: a) Completion of a full comparison between the HESS panel method results and the pressure data previously obtained from wind tunnel measurements performed on the model of a typical twin engine GA airplane (Gruman Cougar) ; b) Modelling of the three dimensional flow about the same airplane model using a state of the art panel method (VSAERO code); c) Testing of the incompressible Navier-Stokes solution method discussed in the progress report for last reporting period for several two dimensional configurations.

a) A complete comparison between the wind tunnel pressure measurements for the above described model and the results obtained from the HESS panel method has been made. This comparison was done in order to investigate the applicability of a widely used panel method to the problem of flow prediction for highly complicated three dimensional aircraft configurations. A reasonably realistic result from the HESS code would make the rather costly Navier-Stokes calculations unnecessary. However, as expected, the HESS code gave good predictions of the flow behavior only at low angles of attack, and even here the detailed information about the flow in the wing-fuselage-flow energizer region was missing. Without this information, a qualitative analysis of the physical phenomena in this region is ambiguous at best. On the other hand, the predicted pressures for the low angles of attack agreed reasonably well with the experimental data. At high angles of attack ($\alpha > 10^{\circ}$) the flow about a major portion of the wing is dominated by separation, so that the pressure results from the panel method were highly inaccurate. The influence of the flow energizers on the flow behavior in regions close to them was also modeled inadequately. Here the wind tunnel measurements clearly displayed a small but noticeable change in local flow behavior after the energizers were added. The predicted results showed essentially no change in pressures at the same locations .

Thus, it was concluded that for overall flow characteristics at low or moderate angles of attack, the HESS code gives good results. However, at high angles of attack, studied in the present research effort, the HESS code proved to be an inadequate tool for analytical investigation of the flow phenomena. The lack of detailed flow description is another obvious shortcoming of this method.

b) In order to further test the usefulness of panel methods for studying behaviours of flows about multiple body configurations at high angles of attack, use is being made of a more modern and well developed panel method code, the VSAERO. Not only does this code handle potential flow about arbitrary three dimensional lifting and non lifting bodies, but it also includes viscous and separated flow effects as well as wake effects. It was felt that this code might be able to model the overall flow behaviour at high angles of attack and account for the local effects of the flow energizers much better than the HESS code. So far, only a small number of initial test case results were obtained.

c) Work on the development of the incompressible Navier-Stokes solver is proceeding steadily. Its implementation for two dimensional flows was first successfully tested on the flat plate boundary layer problem and was subsequantly applied to the viscous flow around a circular cylinder. The highly complicated, separated flow in the case of the cylinder for Re=40 represents an adequate challenge and was predicted by the scheme very well. The pressure data as well as the extent of the separated region agreed very well with experimental and numerical data available in literature. The plot of the resulting velocity vectors in Fig.3 shows the extent and shape of the separated wake region behind the cylinder. From these test cases, an understanding of the behaviour of the scheme in terms of it's stability properties, convergence histories and ability to predict complicated flows correctly was obtained. Several more efficient versions of the basic algorithm were investigated, however, it was found that only its full form had the desired properties. The proper choice of user selectable parameters such as time step Δt, artificial compressibility factor β and coefficients of high frequence filtering α_i and α_e was explored and their optimum values found. Currently, the numerical method is being used for flow predictions about two dimentional incompressible viscous airfoils at moderate and high angles of attack. Concurrently, the method is being extended to three dimensions, so that, in the foreseeable future, the method will be tested on simple three dimensional configurations. It should be pointed out that the availability of a super computer system, provided to us by NASA Langley Research Center was absolutely essential in obtaining these results and will be a must in the case of the three dimensional calculations.

In summary, this part of TASK A is progressing at good pace. The results obtained by the incompressible Navier-Stokes solver so far are very promising. The main objectives of this reseach should be achieved according to our schedule.

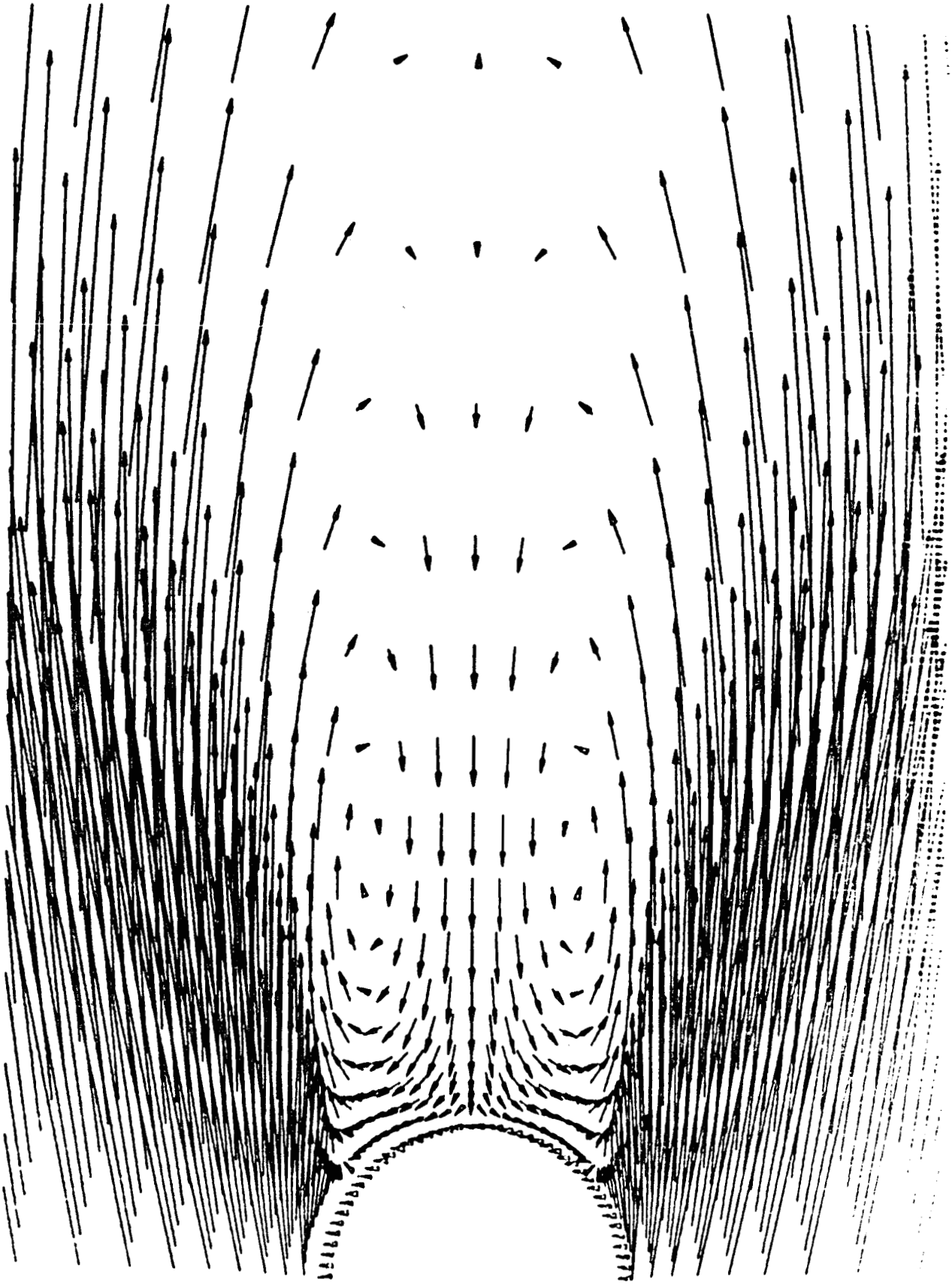

Fig. 3: Wake flow behind a 2-D cylinder at $Re_D = 40$.

TASK B

Slipstream Effects on Natural Laminar Flow

Progress Report

by

S.J. Miley and R. Howard

Aerospace Engineering Department
Texas A&M University
College Station, TX 77843

Sumbitted to Langley Research Center
Hampton, Virginia
Technical Monitor: J. Stickle
Grant No.: NAG 1-344

TASK B: SLIPSTREAM EFFECTS ON NATURAL LAMINAR FLOW

Experimental

The natural laminar flow test glove has been flown on the Schweizer 2-32 sailplane. Aircraft flying qualities were unaffected. Due to inexperience with the use of hot-wire contouring of the foam structure, the upper surface of the glove had large deviations from the template profile. This has resulted in a considerable amount of time expended on filling and sanding to bring the contour to the desired shape. This process is almost completed. Final filling and smoothing is in progress using a wave gauge to control deviations in the measurement area. A 4-channel instrumentation analog tape recorder has been acquired through university cost-sharing. The instrumentation and data acquisition system is presently being installed in the sailplane. Data flights will be initiated in July.

Fabrication of the wind tunnel test model is nearing completion. The model consists of a central steel tube with sections from a helicopter rotor blade attached for the wing structure. A foam/fibreglass outer wing structure will be bonded to the rotor blade sections to obtain the desired wing profile. The outer wing structure is being formed utilizing molds provided by NASA. The central tube has been formed into a clamp which will hold the NASA SR-2 propeller test rig. The tube clamping system will allow a quick change from tractor to pusher configuration without removing the model from the supports in the test section. The inboard section of the wing outer structure will be removable so as to enable both direct sectional drag force measurements and static pressure measurements to be made. A tunnel entry in early August is planned following the NASA SR-2 test program.

Analytical

A literature search was performed on the subject of external turbulence effects on the boundary layer. Most of the activity sin this area is Russian, and is concerned with heat transfer. Comparisons of our measurements in the 2'x3' tunnel with the Russian data reinforce the present slipstream/boundary layer interaction model. The boundary layer cycles through changes in character consistent with periodic changes in external flow turbulence. In the laminar flow region, the boundary layer does not become turbulent as origionally thought, but does contain a region of turbulence near the wall which varies with the external flow turbulence. When comparing velocity profile shape parameters, the profiles with external turbulence become fuller and appear similar to laminar profiles with suction, i.e., profiles having a high degree of stability. Based

upon shape parameter comparisons with laminar and turbulent correlation curves, the external turbulence profiles lie in a transitional region between the two. The possibility of a transitional correlation curve is suggested. This possibility is further inhanced by considering relaminarization profiles which follow the same path as the external turbulence profiles.

Two technical papers have been generated to date. The first paper was presented at the SAE Business Aircraft Meeting in April, 1985, the second is to be presented at the Notre Dame Low Reynolds Number Airfoil Conference in June, 1985. A third paper has been accepted for the AIAA Applied Aerodynamics Conference in October, 1985. Copies of the first two papers are enclosed.

TASK C

Experimental/Computational Study of Minimum Induced Drag and Static Longitudinal Stability For a Three Lifting Surface Configuration.

Progress Report

by

C. Ostowari and D. Naik

Aerospace Engineering Department
Texas A&M University
College Station, Texas 77843

Submitted to Langley Research Center
Hampton, Virginia
Grant Monitor: J. Stickle
Grant No.: NAG 1-344

Overview of Research

A series of wind tunnel experiments have been carried out to investigate the minimum induced drag and static longitudinal stability for a three-lifting surface configuration. The results are compared with the theoretical predictions of previous researchers, especially Butler[1] and Kendall[2,3]. Currently the research is being directed towards obtaining some comparative data from a panelized version of the wind tunnel model, run on the VSAERO code.

Objective

The theories and modifications to the theories of Prandtl and Munk have been used by a number of researchers to explore the minimum induced drag of multiplanes (aircraft with multiple wings). These studies have yielded comparative predictions of the induced drag and static longitudinal stability of conventional aircraft, canard aircraft and three surface aircraft. The effect of variations in gap and stagger are also an integral portion of these studies.

Kendall has summarized the analytical results, theorizing that minimum induced drag should be attainable at any centre of gravity (cg) location so long as equal and opposite vertical loads are applied by the forward and aft lifting (or trimming) surfaces. Furthermore, these minimum induced drag loads should be achievable at any useable cg location, within the practical limits set by the size and shape of the lifting surfaces.

An important and pragmatic concern about these theoretical studies is that idealizing assumptions have been made, usually closely allied to Prandtl's and Munk's assumption of an elliptical spanwise lift distribution. Butler, among others, has suggested that for non-elliptical lift distributions with pure canards, the effects are significantly different from idealised theory. He also predicts that the three surface induced drag at both typical cruise and high lift conditions is lower than the induced drag of either a conventional aircraft or a canard-wing type.

This study examines these theoretical studies in the light of aerodynamic force and moment measurements of a typical business jet aircraft that is modified by the addition of a forward wing and fuselage extension for stagger. The study also undertakes a rough comparison with predictions from the VSAERO panel code.

measurement methods to accurately determine transition. Time-dependent behavior, particularly at frequencies associated with propeller blade passage rate, was not measurable by techniques commonly employed at that time. Measurements by Holmes, et al. [7] using surface hot-wire sensors indicate the existence of a cyclic turbulent behavior resulting in convected regions of turbulent packets between which the boundary layer appears to remain laminar (Figure 1).

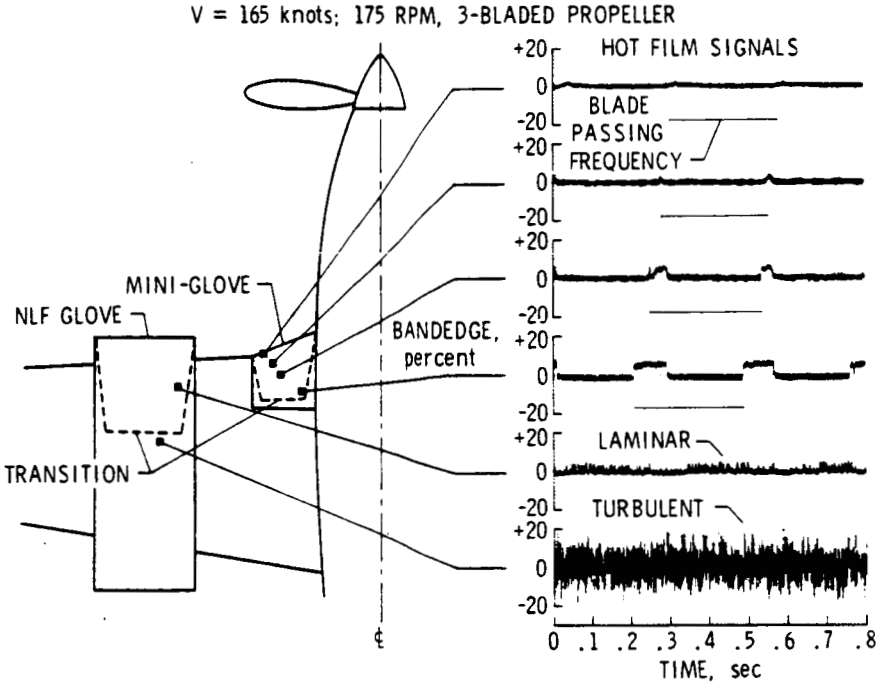

Figure 1. Surface hot-film measurements by Holmes et al. [7] showing cyclic laminar/turbulence behavior of boundary layer within propeller slipstream.

EXPERIMENTAL INVESTIGATIONS

Flight Experiments

At Texas A&M University, flight measurements of the wing boundary layer in the slipstream have been made on a Gulfstream Aerospace GA-7 Cougar at two chord locations using a dual-probe hot-wire velocity sensing system. One probe was located adjacent to the surface well within the boundary layer and the other was located directly above in the external flow. The results of the flight test are shown in Figures 2-4.

The signal traces are time histories of the local flow velocities in the boundary layer near the surface and in the external flow. The boundary layer velocity signal shows a periodic laminar/turbulent behavior. The change to turbulent flow results in an increase in the velocity seen by the probe because of the fuller turbulent profile. This change in profile results from periodic disturbances in the external flow due to the viscous wake shed from the propeller blade.

Concluding Remarks

Preliminary experimental results indicate broad agreement with Butler's conclusions on the induced drag. Currently the analytical study is underway and results should be available shortly. Final conclusions will appear in the form of a journal article. However, the full complement of wind tunnel test data is given in the Appendix.

References

1. Butler, G. F., "Effect of Downwash on the Induced Drag of Canard-Wing Combinations," Journal of Aircraft, Vol. 19, May 1982, pp. 410,411

2. Kendall, E. R., "The Minimum Induced Drag, Longtidunal Trim and Static Longtidunal Stability of Two-Surface and Three-Surface Airplanes," AIAA paper # 84-2164.

3. Kendall, E. R., "The Aerodynamics of Three-Surface Airplanes," AIAA paper # 84-2508.

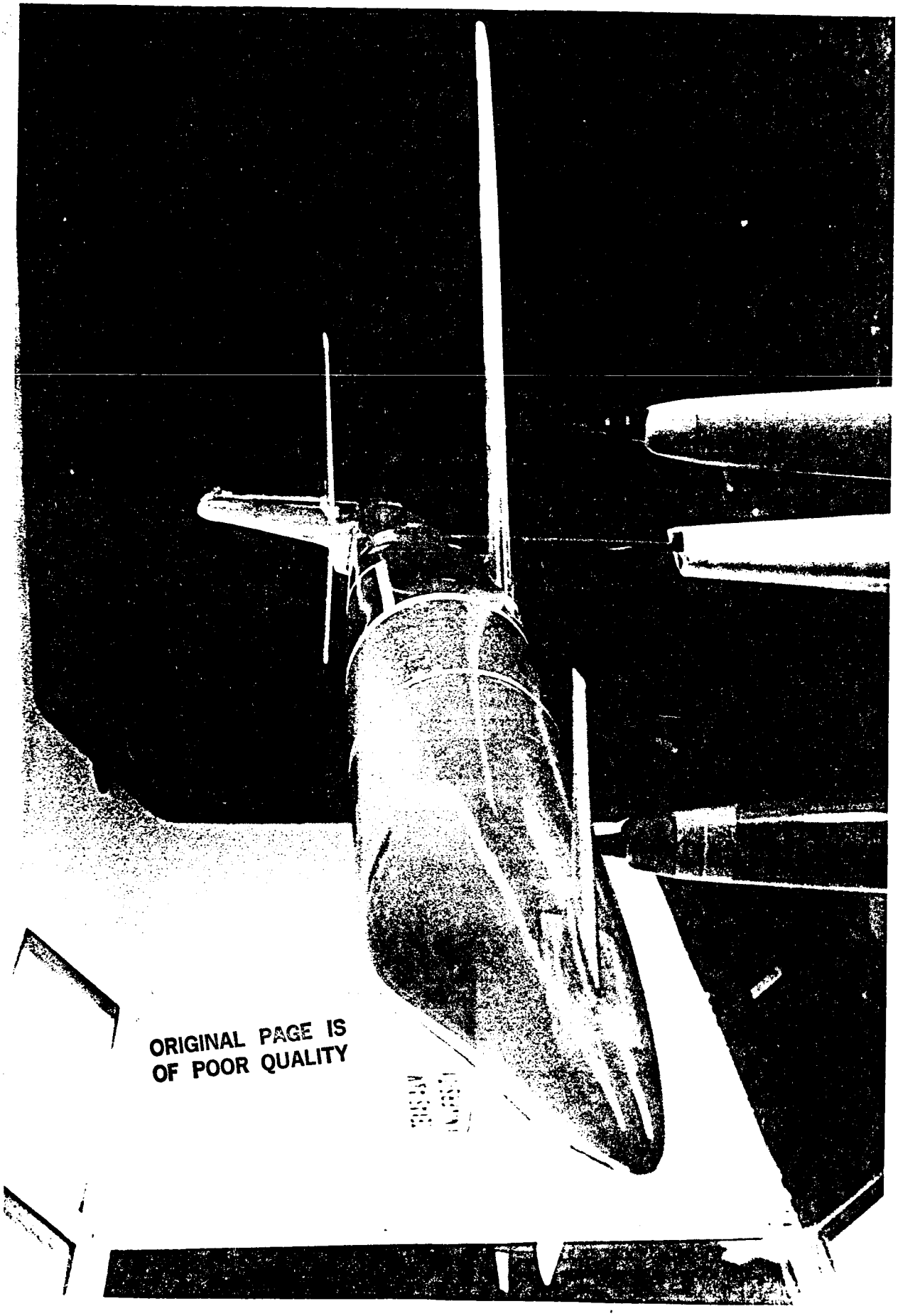

ORIGINAL PAGE IS
OF POOR QUALITY

Figure 1 - Three-Lifting Surface Model in the 2.13 m x 3.05 m wind tunnel. The fuselage plug is bounded by the light bands in the photograph.

ORIGINAL PAGE IS
OF POOR QUALITY

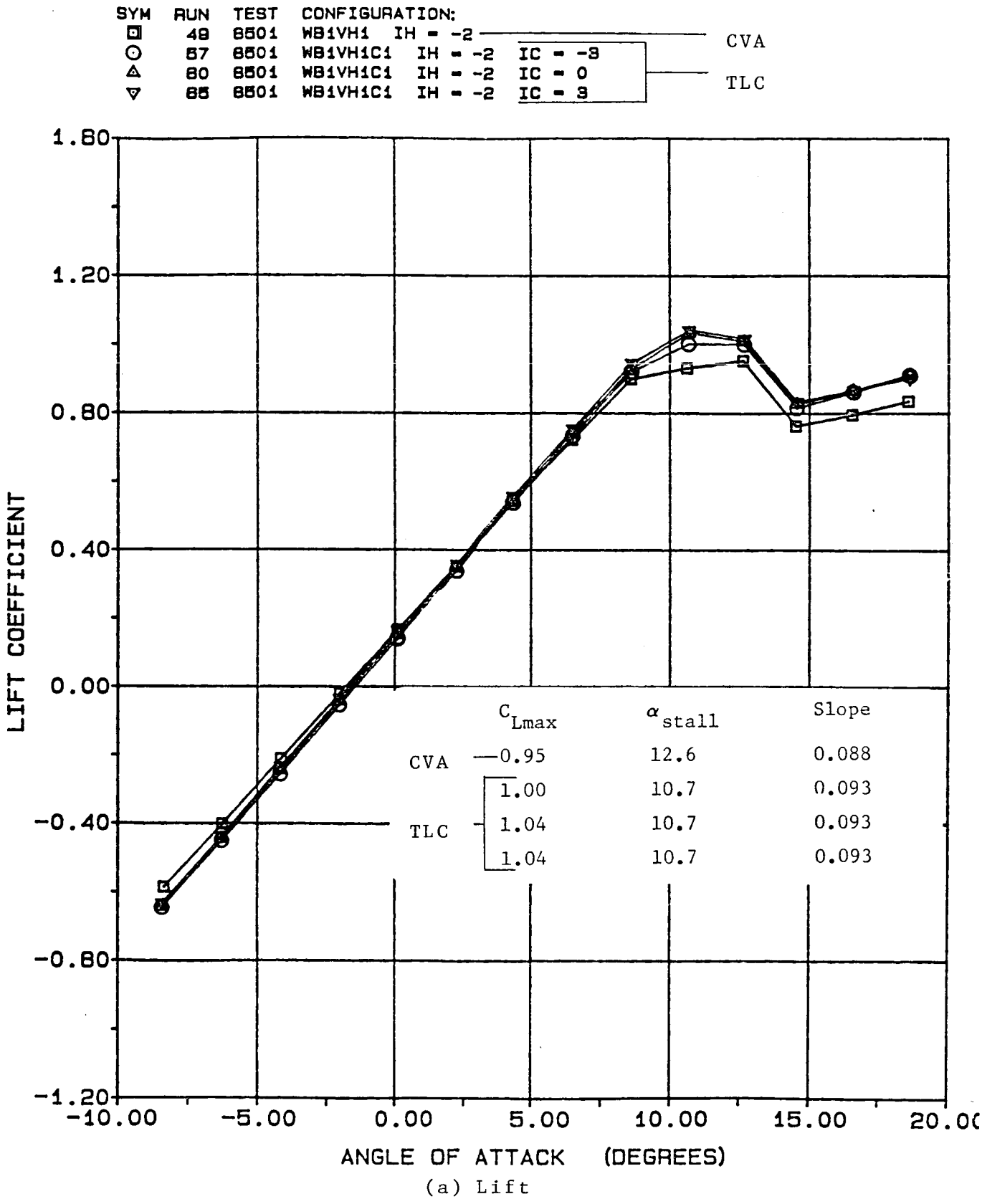

(a) Lift

Figure 2 - Comparison between a TLC and a CVA. Short body, High horizontal tail, large forward wing.

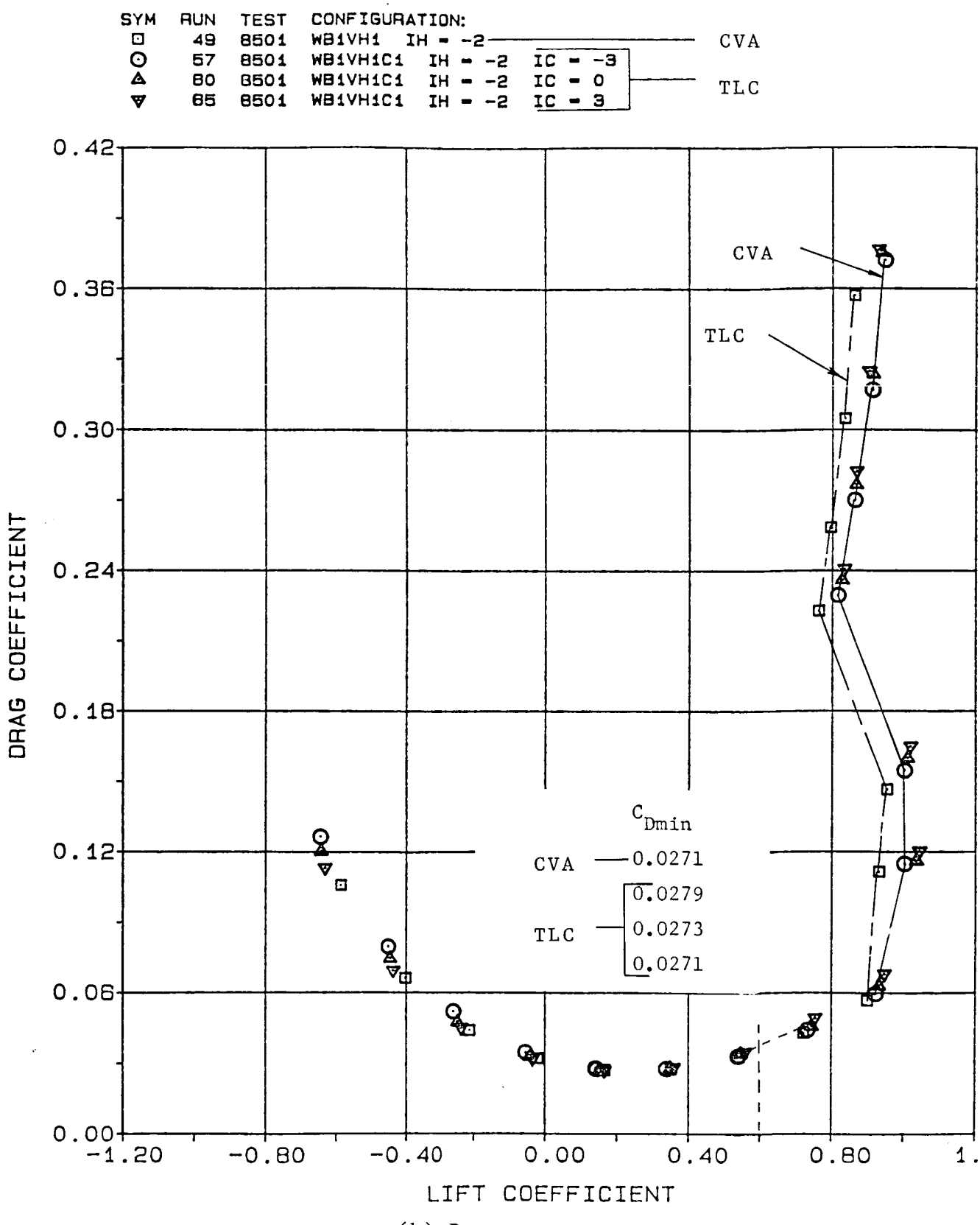

(b) Drag

Figure 2 - Continued.

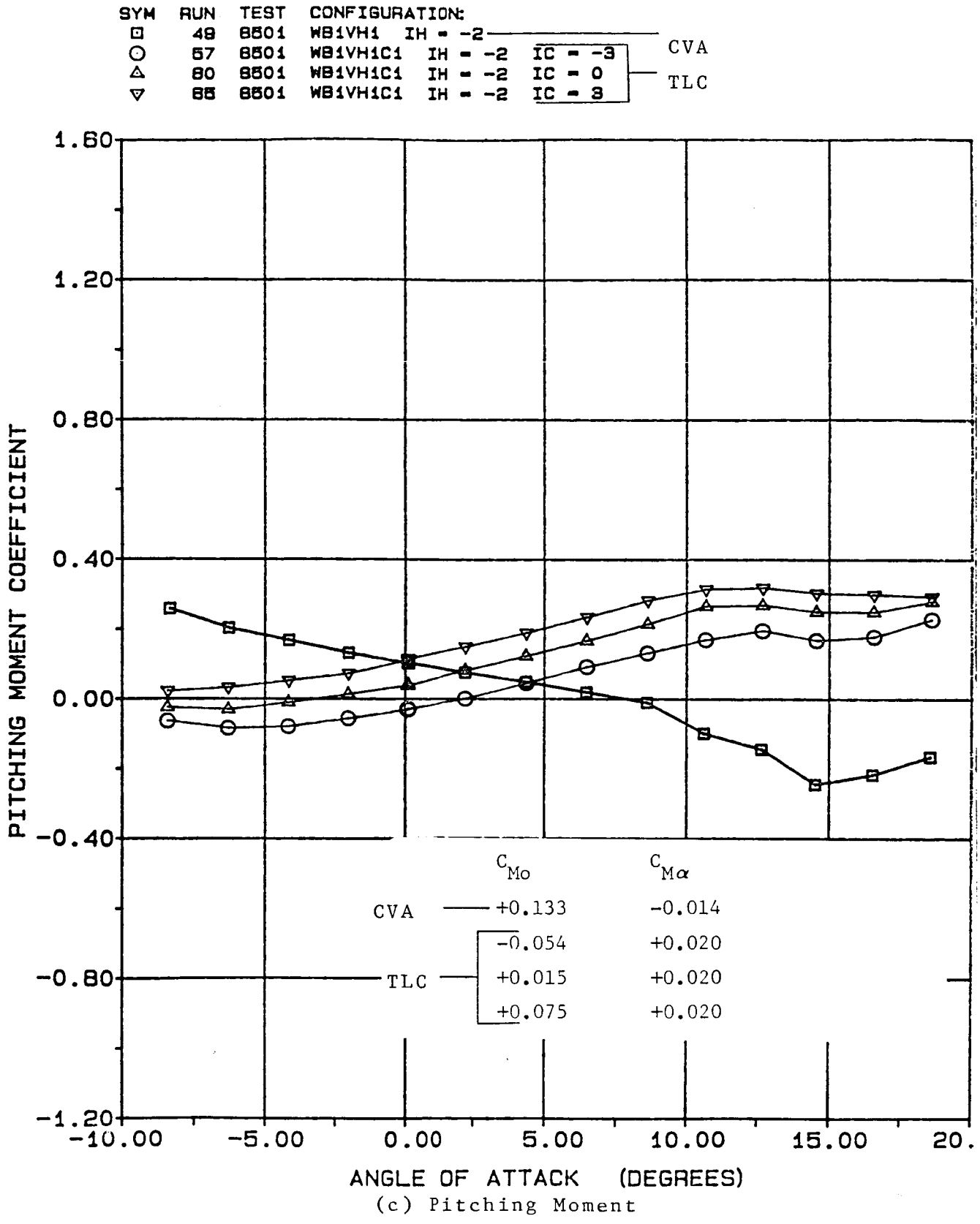

(c) Pitching Moment

Figure 2 - Concluded.

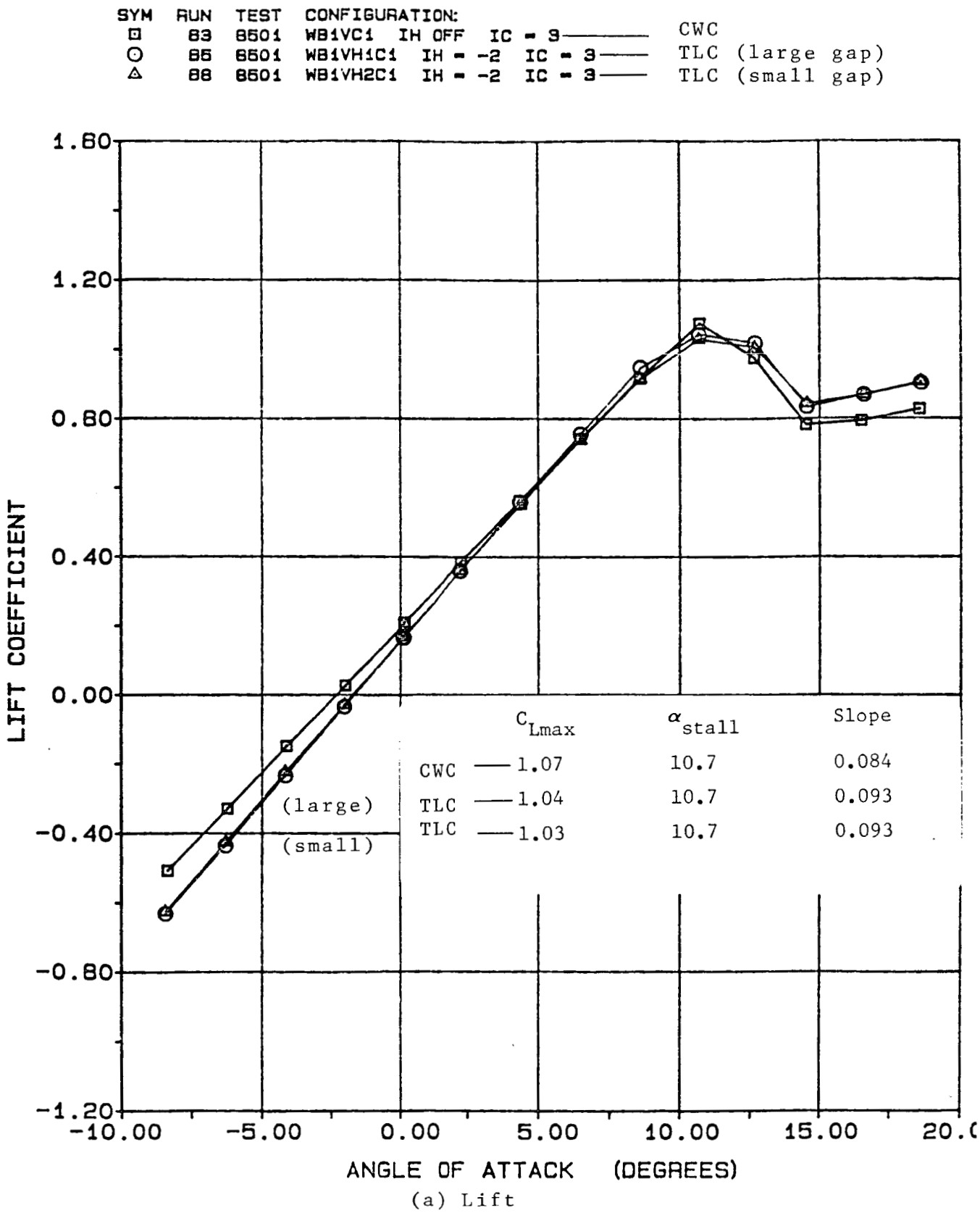

(a) Lift

Figure 3 - Comparison between a CWC and a TLC. Also shown is the effect of a change in gap.

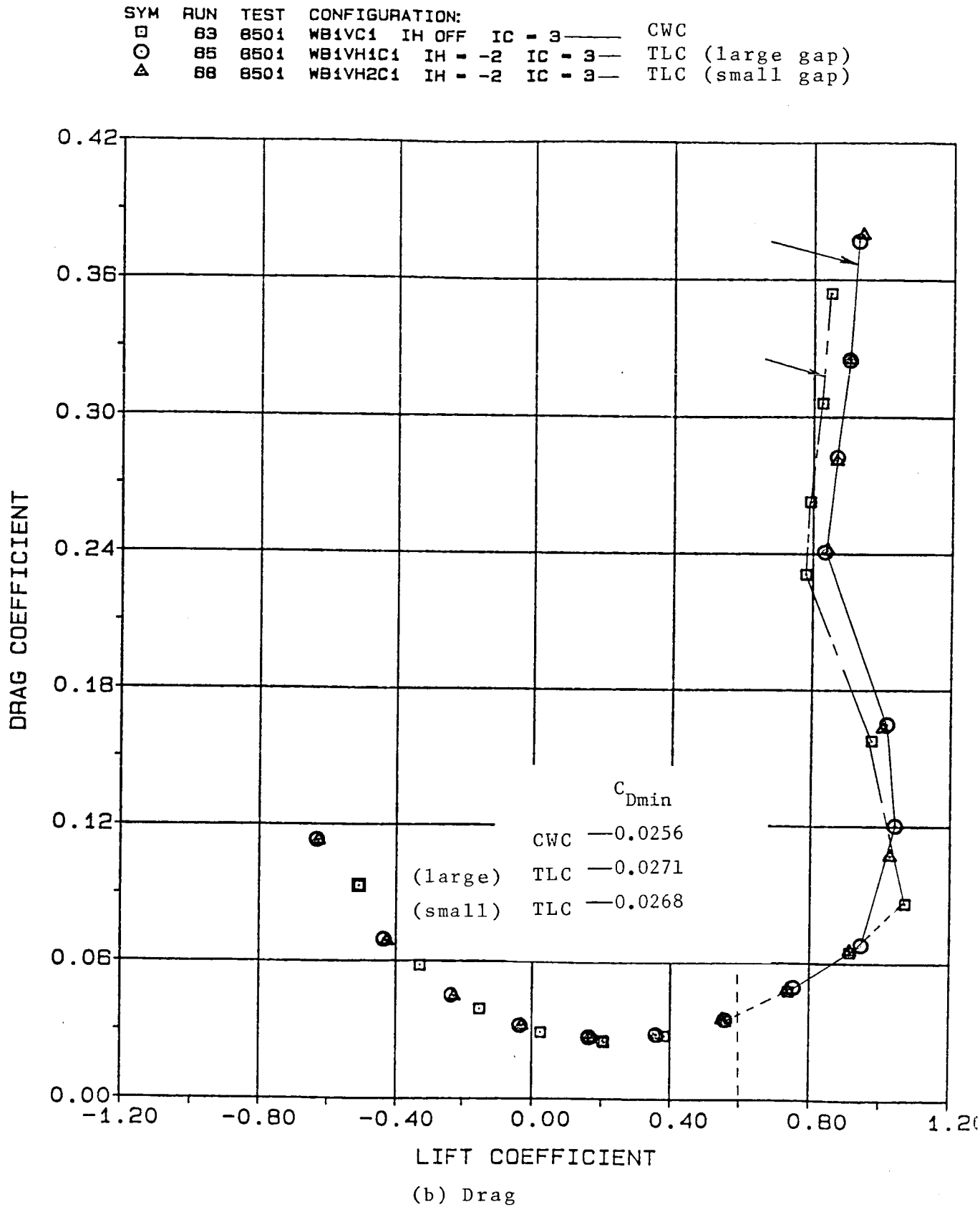

(b) Drag

Figure 3 - Continued.

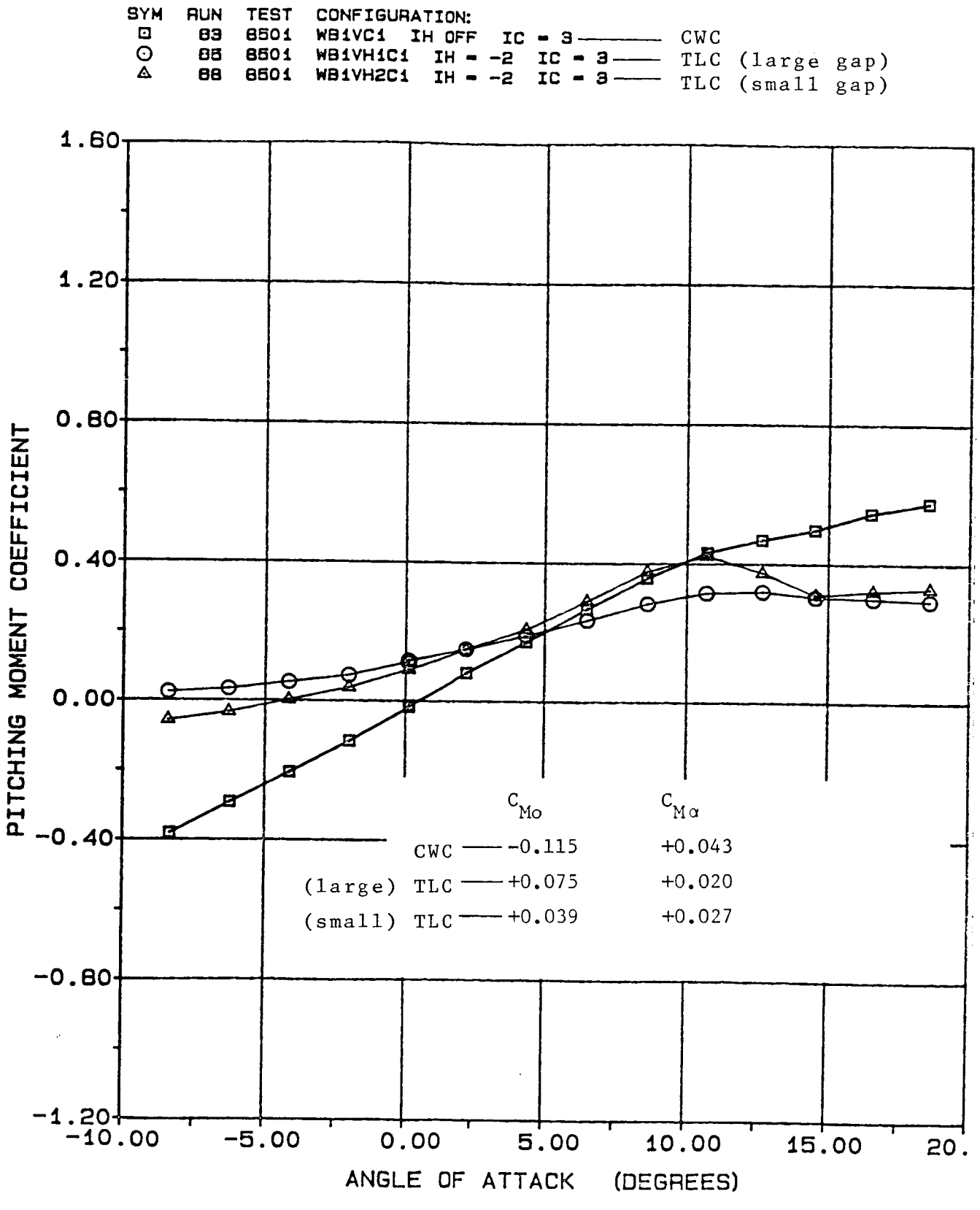

(c) Pitching Moment

Figure 3 - Concluded.

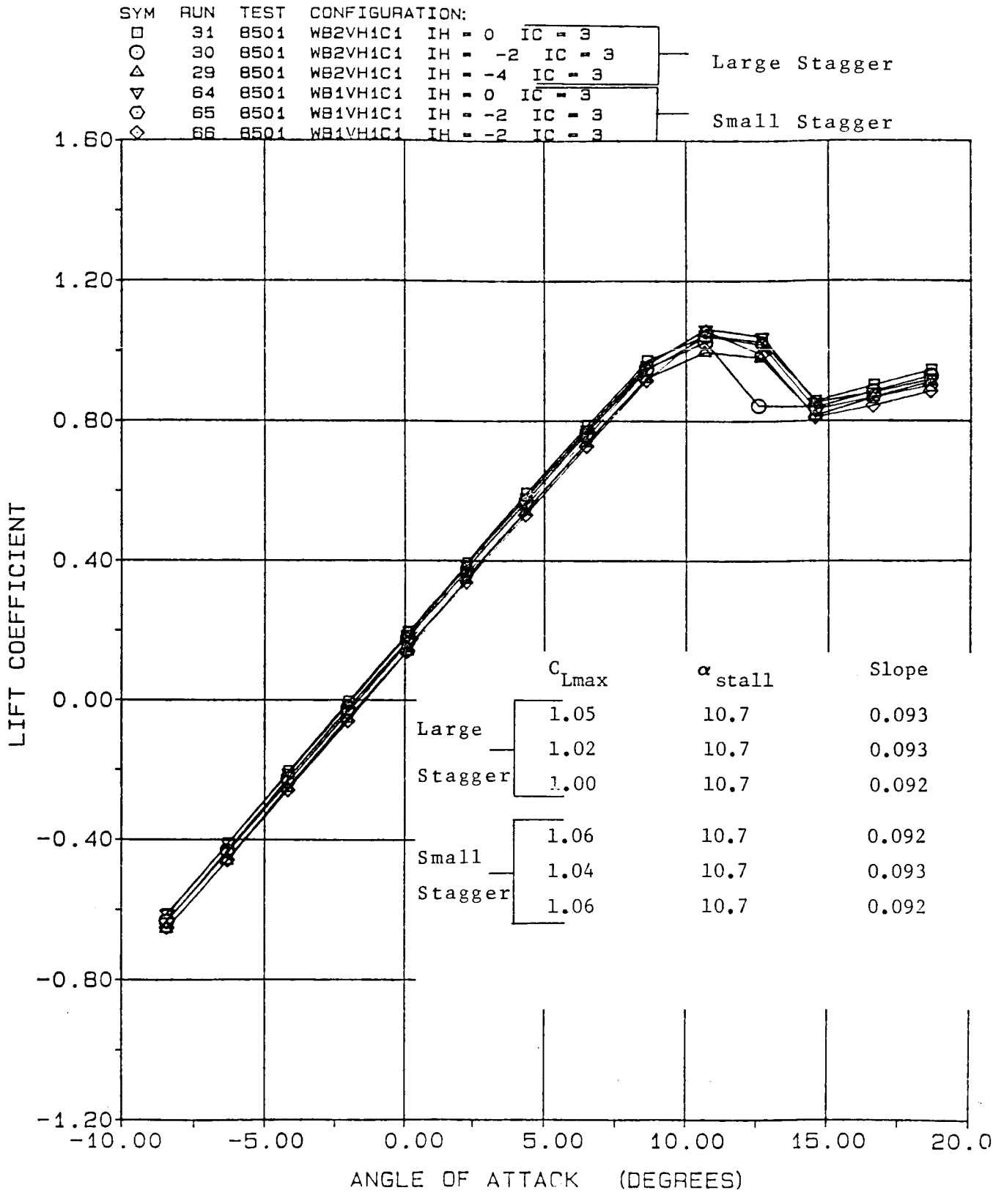

(a) Lift

Figure 4 - The effect of stagger on the aerodynamic coefficients of a TLC.

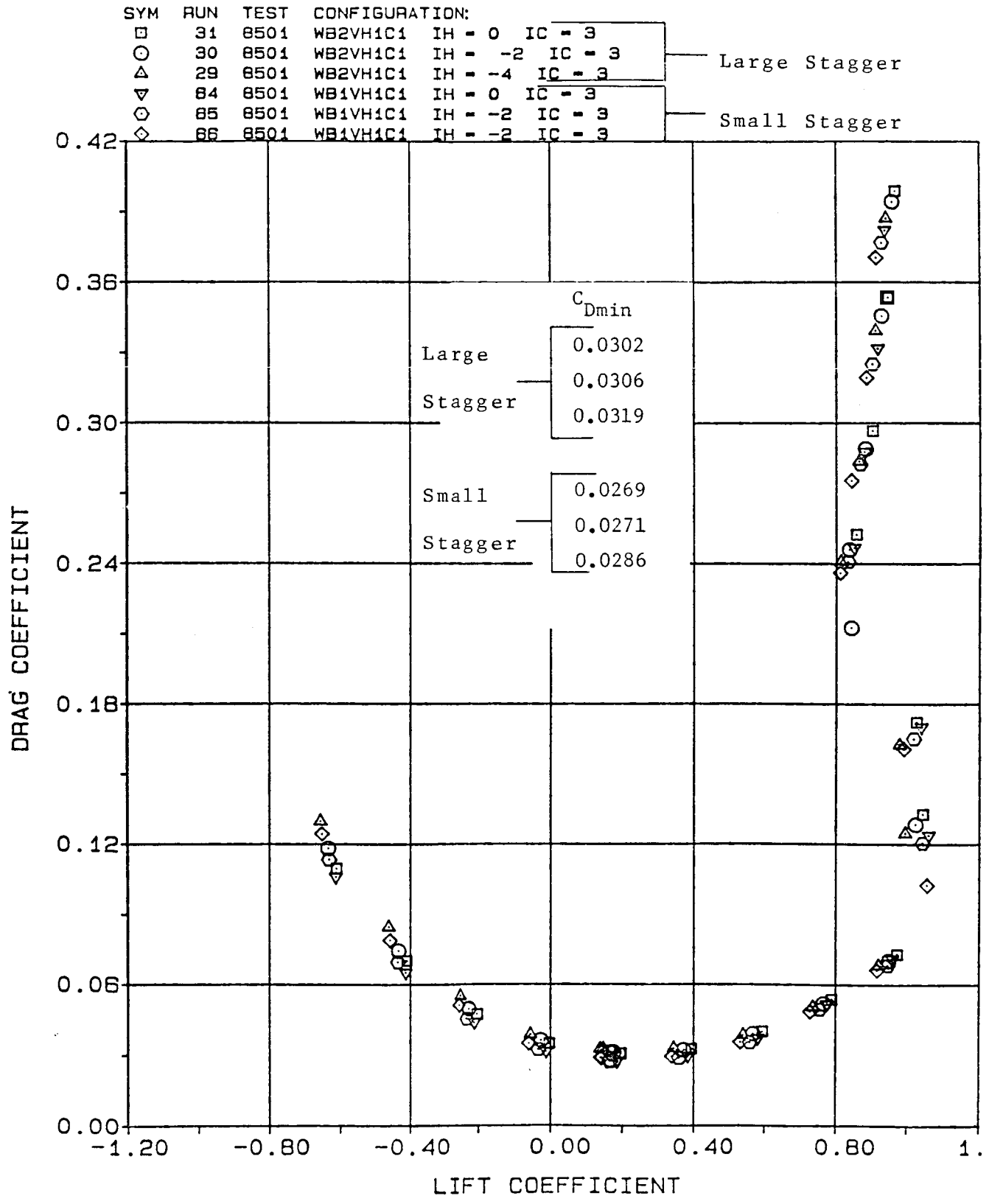

(b) Drag

Figure 4 - Continued.

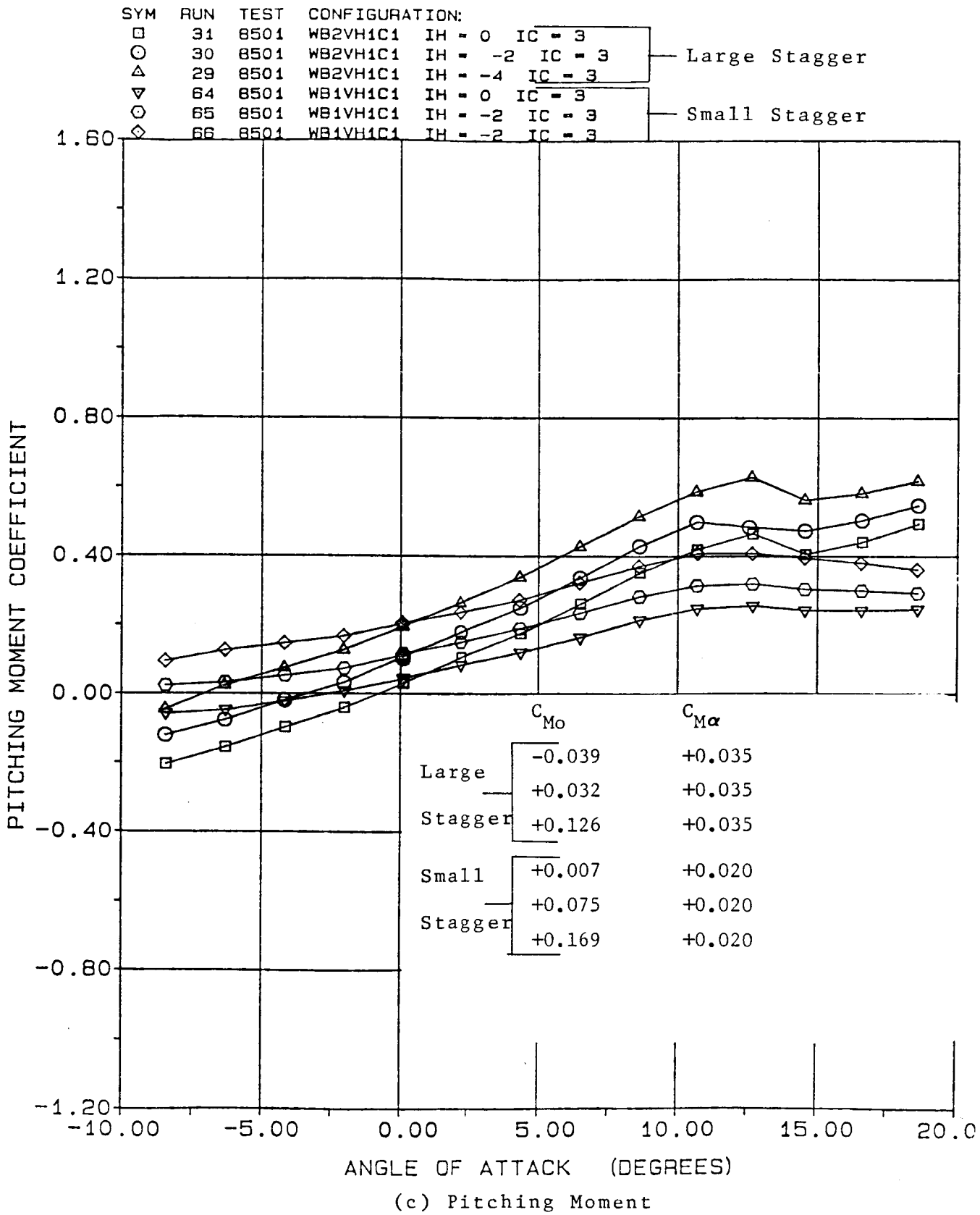

(c) Pitching Moment

Figure 4 - Concluded.

SAE The Engineering Resource For Advancing Mobility
400 COMMONWEALTH DRIVE WARRENDALE, PA 15096

SAE Technical Paper Series

850859

An Investigation of the Effects of the Propeller Slipstream on a Laminar Wing Boundary Layer

Richard M. Howard and Stan J. Miley
Texas A&M University
Bruce J. Holmes
NASA Langley Research Center

Reprinted from SP-621—
General Aviation Aircraft Aerodynamics

General Aviation Aircraft
Meeting and Exposition
Wichita, Kansas
April 16-19, 1985

Copyright 1985 Society of Automotive Engineers, Inc.

This paper is subject to revision. Statements and opinions advanced in papers or discussion are the author's and are his responsibility, not SAE's; however, the paper has been edited by SAE for uniform styling and format. Discussion will be printed with the paper if it is published in SAE Transactions. For permission to publish this paper in full or in part, contact the SAE Publications Division.

Persons wishing to submit papers to be considered for presentation or publication through SAE should send the manuscript or a 300 word abstract of a proposed manuscript to: Secretary, Engineering Activity Board, SAE.

Printed in U.S.A.

850859

An Investigation of the Effects of the Propeller Slipstream on a Laminar Wing Boundary Layer

Richard M. Howard and Stan J. Miley
Texas A&M University
Bruce J. Holmes
NASA Langley Research Center

A research program is in progress to study the effects of the propeller slipstream on natural laminar flow. Flight and wind tunnel measurements of the wing boundary layer have been made using hot-film velocity sensor probes. The results show the boundary layer, at any given point, to alternate between laminar and turbulent states. This cyclic behavior is due to periodic external flow turbulence originating from the viscous wake of the propeller blades. Analytic studies show the cyclic laminar/turbulent boundary layer layer to result in a significantly lower wing section drag than a fully turbulent boundary layer. The application of natural laminar flow design philosophy yields drag reduction benefits in the slipstream affected regions of the airframe, as well as the unaffected regions.

IT IS BECOMING increasingly apparent that natural laminar flow (NLF) is a technology whose time has come to the general aviation industry. What had been the exclusive province of high performance sailplanes, is now commonplace in sport aircraft and is appearing on advanced technology prototype business aircraft. The adoption of NLF methodology brings numerous design problems in the general area of aerodynamic cleanliness. An important design problem for propeller driven aircraft is where to put the propeller slipstream. Tractor propeller installations offer many adntages. A generally accepted disadvantage, however, is that the propeller slipstream will come in contact with some parts of the airframe and eliminate the beneficial effects of laminar flow from the affected areas. The commonly applied solution is to adopt pusher installation designs to remove the slipstream from contact with the airframe. Pusher installations have their disadvantages also, however. In a recent survey of propeller propulsion integration technology by Miley and von Lavante (1)*, no clear advantage was found in the comparison of tractor versus pusher wing mounted installations. This conclusion is based upon a review of available published data from 1930 to present. As part of the Viscous Drag Reduction Research Program at NASA Langley Research Center, Texas A&M University (TAMU) has been investigating the effects of a propeller slipstream on natural laminar flow.

Early observations of the effect of the propeller slipstream on boundary layer transition have not resulted in consistent conclusions. Young and Morris (2,3), and Hood and Gaydos (4) concluded from their investigations that in the propeller slipstream the point of transition from laminar to turbulent flow moved forward to a location near the leading edge. Reports by Zalovcik (5), and Zalovcik and Skoog (6) describe wing boundary layer measurements in propeller slipstreams performed on P-47 aircraft utilizing a NACA 230 series wing section and a NACA 66 laminar flow series wing section. Their results show little effect of the slipstream on transition for the NACA 230 section; however, the test with the NACA 66 series wing section resulted in the transition point location moving forward from 50 percent to 20 percent chord, indicating a significant loss of laminar flow.

* Numbers in parentheses designate references at end of paper.

Recent work by Holmes, Obara and Yip (7) and Holmes, et al. (8) brings into question the validity of the ability of the early measurement methods to accurately determine transition. The use of total pressure probes in combination with large volume pressure transducers, such as manometer systems, provided only time-averaged information. Time-dependent behavior, particularly at frequencies associated with propeller blade passage rate, was not measurable by techniques commonly employed at that time. Measurements by Holmes, et al. (7) using surface hot-film sensors indicate the existence of a cyclic turbulent behavior resulting in convected regions of turbulent packets between which the boundary layer appears to remain laminar. The observed behavior is summarized in Figure 1.

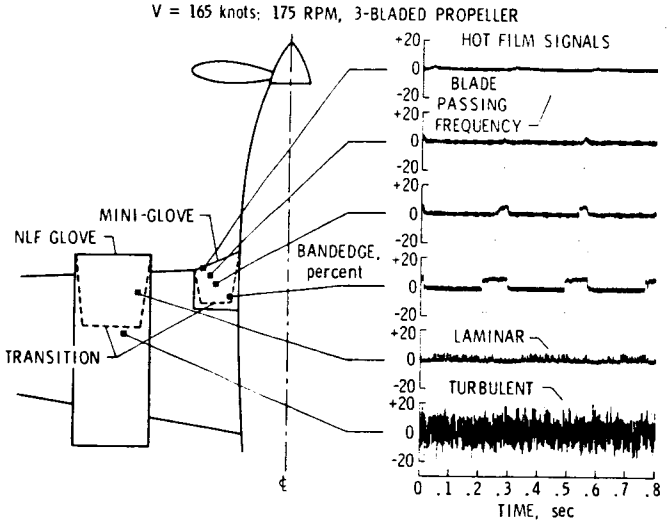

Figure 1. In-flight, hot-film measured, time-dependent effects of propeller slipstream on the laminar boundary layer (T34C airplane).

The present research program at TAMU is extending the initial work by Holmes, et al. towards a more detailed study of the response of the laminar boundary layer to the propeller slipstream. Analysis of the discovered periodic laminar/turbulent nature of the wing boundary layer forms the basis of the current effort. The ultimate objective of this effort is to develop a practical means for predicting skin friction drag on laminar surfaces immersed in propeller slipstreams. In the case of wing sections, the results of the study may lead to airfoil designs which utilize the slipstream affected boundary layer to advantage.

EXPERIMENTAL INVESTIGATIONS

FLIGHT EXPERIMENTS - Initial experiments at TAMU were carried out in flight on a Gulfstream Aerospace GA-7 Cougar donated to the university by Gulfstream for faculty and student research projects. A two-probe hot-film velocity sensing system was installed on the wing within the slipstream at two different chordwise locations. One probe was located adjacent to the surface, well within the boundary layer. The second probe was mounted directly above, outside of the boundary layer, in the external flow. The signals recorded simultaneously provide an indication of the external flow disturbance and the subsequent boundary layer response to this disturbance. A constant power setting was used, and the airspeed was varied over the operating range of the aircraft. The engine on the instrumented side was shut down and the test conditions were repeated under asymmetrical power to record the flow behavior without the slipstream disturbance.

FLIGHT RESULTS - The results of this investigation are given in Figures 2-4. The signal traces are time histories of the local flow velocity in the boundary layer near the surface and in the external flow immediately above the boundary layer. It is noted here that the noise in the laminar signals is due to structural vibration associated with engine and propeller operation. The boundary layer velocity signal shows a periodic laminar/turbulent flow. The change to turbulent flow results in an increase in the velocity seen by the probe because the corresponding turbulent boundary layer velocity profile is fuller near the surface. The turbulent flow in the boundary layer results from periodic disturbances in the external flow due to the viscous wake from the propeller blade. The length to which the cyclic turbulence remains in the boundary layer is dependent upon local laminar stability. At the high-speed end, the pressure gradient is strongly favorable, and laminar stability is correspondingly high. Here, the boundary layer reverts almost immediately back to laminar flow after the passage of the external disturbance. At the low-speed end, the pressure gradient is no longer strongly favorable, laminar stability is greatly decreased, and the turbulence remains for almost the total cycle.

The corresponding character of the boundary layer flow without the propeller running is shown in Figure 3. The wing section of the GA-7 is a NACA 64 laminar flow series. At low angles of

ORIGINAL PAGE IS
OF POOR QUALITY

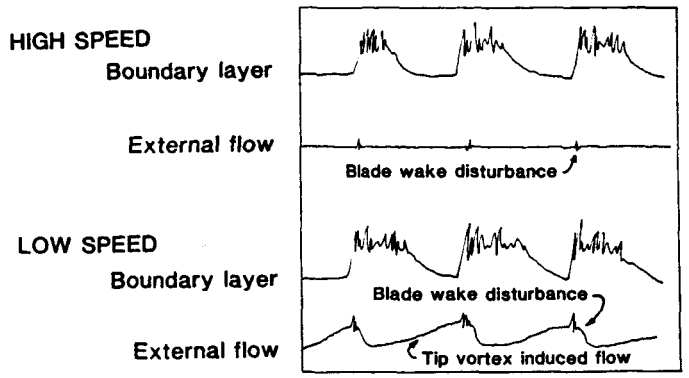

Figure 2. Description of velocity sensor signals seen in Figures 3 and 4.

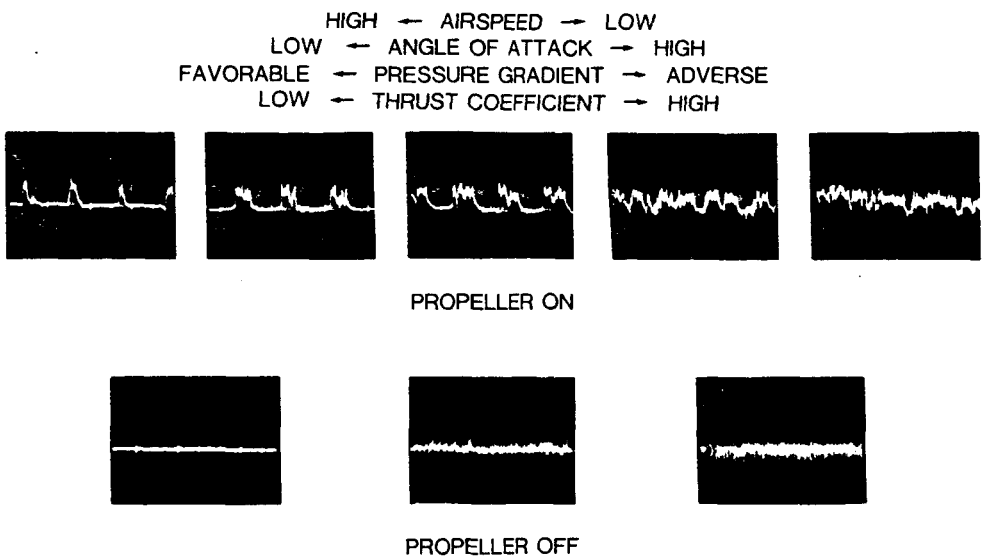

Figure 3. Time-dependent boundary layer velocity response with and without slipstream measured in flight at 12 percent chord.

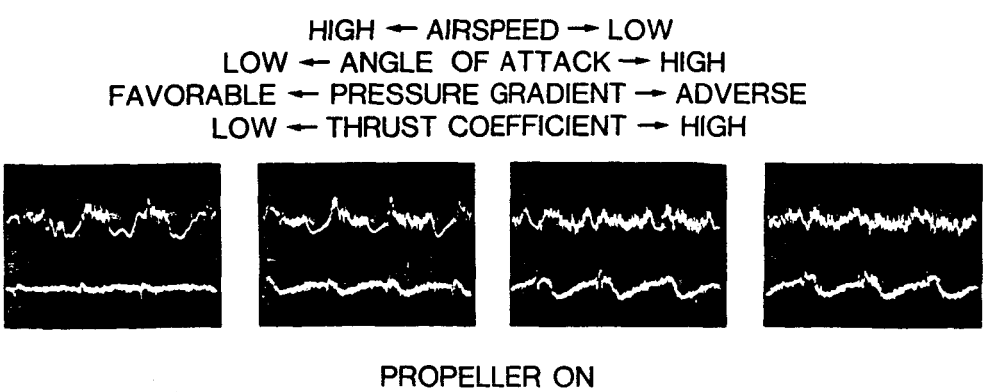

Figure 4. Time-dependent boundary layer and external flow velocity response with slipstream measured in flight at 30 percent chord.

attack, a favorable pressure gradient normally extends to 40 percent chord. However, away from the leading edge, the pressure distribution flattens out giving a less favorable pressure gradient. This, in combination with the growth of the boundary layer, progressively reduces laminar stability, eventually leading to transition and turbulence. These results imply that more strongly favorable pressure gradients will be required to achieve maximum runs of laminar flow in propeller slipstreams. The effects of reduced laminar stability at the 30 percent chord location is evident in Figure 4. Here also is seen the character of the external flow disturbance due to the propeller slipstream. The viscous blade wake appears as short wave impulse barely discernible at the high speed end. As the speed is reduced, the propeller blade operates at an increasingly higher angle of attack and the viscous wake grows, leading to a more pronounced impulse disturbance signal. This is noted in the figures in terms of the propeller thrust coefficient. The low frequency wave pattern which develops in the external slipstream flow is due to the propeller tip vortex. As demonstrated by Sparks and Miley (9), the helical tip vortex induces an axial component in the slipstream velocity which increases with vortex strength (propeller thrust coefficient), and as the edge of the slipstream boundary is approached. While the tip vortex induced flow dominates the slipstream velocity signal, it will be shown that it is the relatively smaller blade viscous wake disturbance which is affecting the laminar boundary layer.

A slipstream disturbance flow model was constructed from analyzing the flight data, and is shown in Figure 5. The viscous wake from the propeller blade forms a helical sheet which is split by the wing; one part passing over the upper surface, the other part passing over the lower surface. The turbulence in this helical wake is seen by a stationary point in the boundary layer as a periodic change in external flow turbulence. The laminar boundary layer responds by transitioning to the turbulent state, and then returning to the laminar state through reverse-transition based on the degree of local laminar stability. With the knowledge gained from the flight test program, a small-scale wind tunnel program was initiated to study the boundary layer response in more detail.

WIND TUNNEL INVESTIGATION - The investigation was carried out in the TAMU 2 by 3 foot wind tunnel. The test model was a 30-inch chord NACA 0012 composite wing section with an 18-inch diameter single-bladed propeller and electric motor mounted at wing level at one-fifth chord distance upstream. Measurements were made at various angles of attack with a constant temperature hot-wire anemometer system utilizing a dual-probe configuration similar to that of the flight investigation. The probes were installed so that they could be traversed in a chordwise direction along the airfoil. The probe support are was free to pivot so that the sensors followed the airfoil contour, maintaining constant heights of approximately 0.01 inches (.25 mm) and 1.0 inches (25 mm) above the surface. Thus, as in the

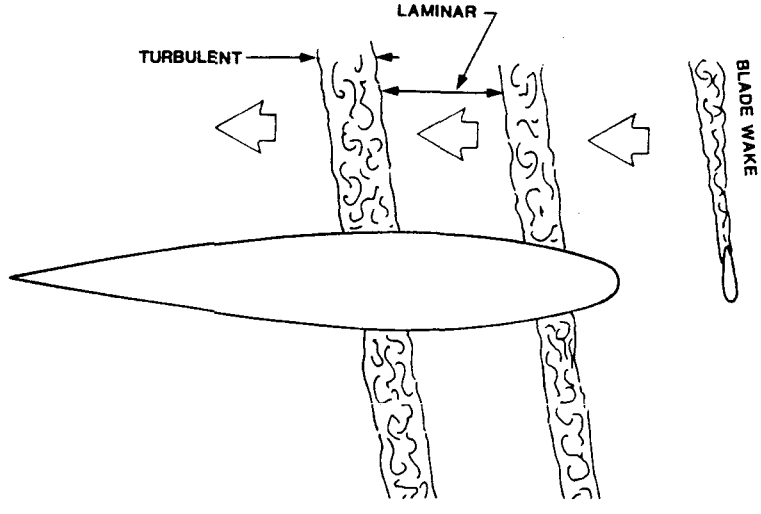

Figure 5. Propeller slipstream disturbance flow model.

ORIGINAL PAGE IS
OF POOR QUALITY

flight investigation, velocity measurements were made in the boundary layer near the airfoil surface and in the external flow.

A second series of experiments was conducted using a mechanism to enable single hot-film probe to traverse the boundary layer normal to the surface. Runs were made at three chord locations and at three angles of attack. The velocity time histories were digitized through a microcomputer and stored on floppy disk for analysis.

Due to the low running speeds of the wind tunnel, the test Reynolds numbers were an order of magnitude lower than the flight measurements. However, similar behavior of the boundary layer to the flight results was observed. The wind tunnel results are therefore taken to be a valid representation of flight behavior insofar as scaling permits.

WIND TUNNEL RESULTS - Two runs from the first series of experiments are shown in Figures 6, 7 and 8. Figure 7 shows a series of measurements at -3 degrees angle of attack, resulting in a favorable pressure gradient along the upper surface. In each photograph the upper trace is the velocity in the boundary layer near the surface; the middle trace is the velocity for the external flow probe; and the lower trace is the trigger signal for the oscilloscope obtained from a magnetic proximity transducer sensing propeller blade passage. The upper row of photographs shows the velocity at chord locations indicated with the propeller off. Transition takes place at approximately 70 percent chord at a chord Reynolds number of 6×10^5. The actual character of the observed transition region is shown in

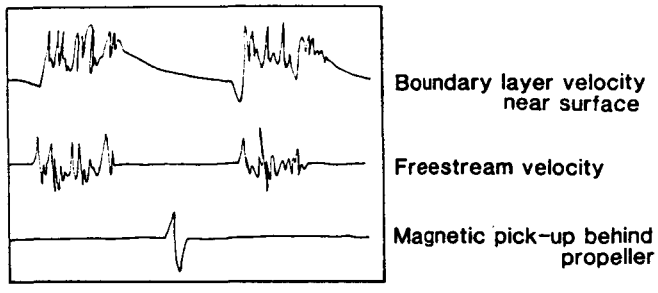

Figure 6. Description of velocity sensor signals seen in Figures 7 and 8.

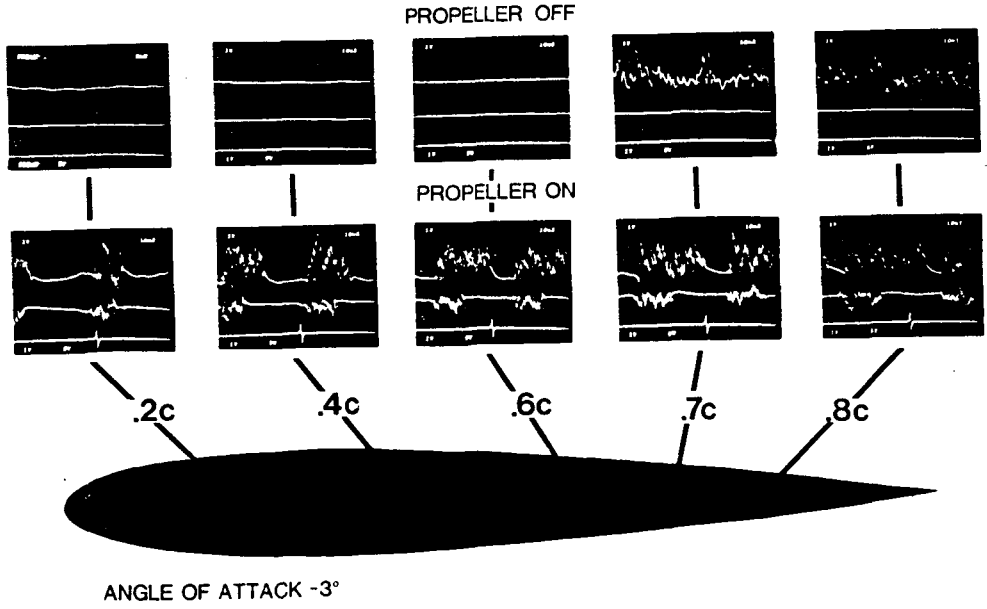

Figure 7. Time-dependent boundary layer and external flow velocity response with and without slipstream measured in the wind tunnel, $\alpha = -3°$.

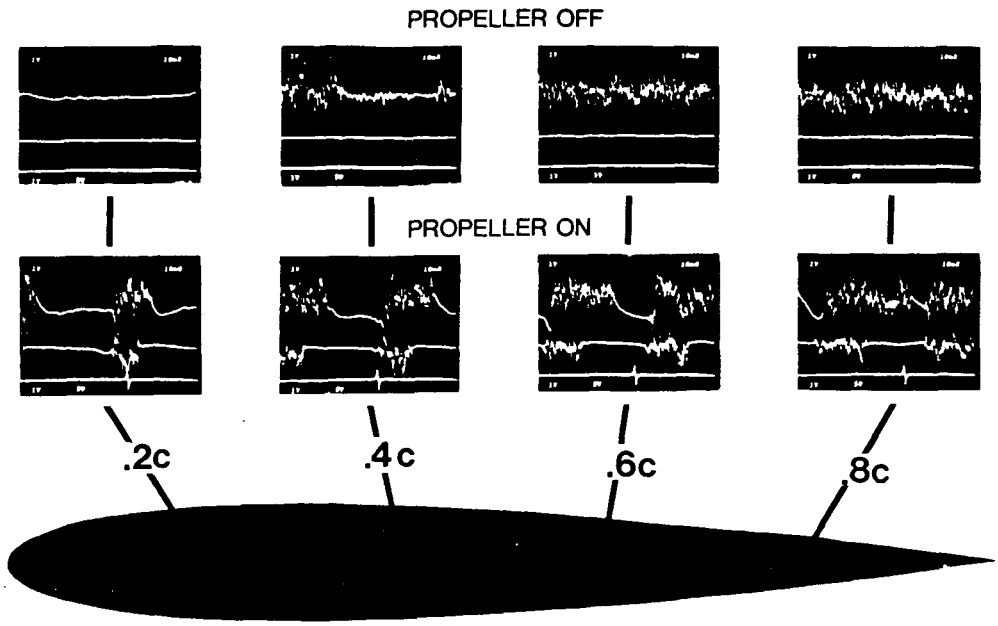

Figure 8. Time-dependent boundary layer and external flow velocity reponse with and without slipstream measured in the wind tunnel, $\alpha=1°$.

the corresponding photograph. Low frequency Tollmien-Schlichting waves appear with intermittent bursts of turbulence.

The lower row of photographs shows the velocities measured with the propeller running. The blade wake in the external flow can be seen in the middle trace and the boundary layer response near the surface in the upper trace. The growth of the turbulent part of the cycle increases with decreasing laminar stability in the chordwise direction. Evident also is cyclic laminar penetration of the previously turbulent region on the aft part of the airfoil. Note this effect in the photograph for the 80 percent chord location. This behavior was seen in the flight data, but it is much more pronounced here; possibly because of the reduced Reynolds numbers. Another important feature is more evident here: the waveform of the cyclic velocity variation. With the arrival of the external disturbance, the velocity at the sensor location immediately jumps to the corresponding turbulent level. After the disturbance passes, the velocity returns to the laminar level as an exponential decay. This behavior will be discussed later in the paper.

Figure 8 shows the results for +1 degrees angle of attack. Outside of an initial favorable gradient peak near the leading edge, the pressure gradient is adverse over the upper surface. The laminar boundary layer responds accordingly, transition now occurring at 40 percent chord. The turbulent length of the cycle behaves as noted previously. More evident here is the cyclic laminar penetration of the previously turbulent boundary layer. For the test Reynolds numbers, the propeller slipstream appears to have a beneficial effect in the turbulent flow region of the airfoil. The mechanism behind the laminar penetration is not understood at present. Likely possibilities include a reaction to the cyclic external flow turbulence, and/or three-dimensional effects from the swirl component in the helical wake sheet. The latter was investigated by orienting the hot-film sensor parallel to the chordwise direcso that the primary response would be in the spanwise or crossflow direction.

The crossflow measurements are shown in Figure 9. The boundary layer velocity in the crossflow direction at the sensor, changes from laminar to turbulent without the increase associated with the change in velocity profile, as observed with the measurements in the chordwise direction. In the external flow, there is a definite vorticity component in the crossflow direction in the blade wake. The direction of the vorticity is consistent with that which would be shed by a propeller blade generating lift. The importance of this effect is not known at present.

ORIGINAL PAGE IS
OF POOR QUALITY

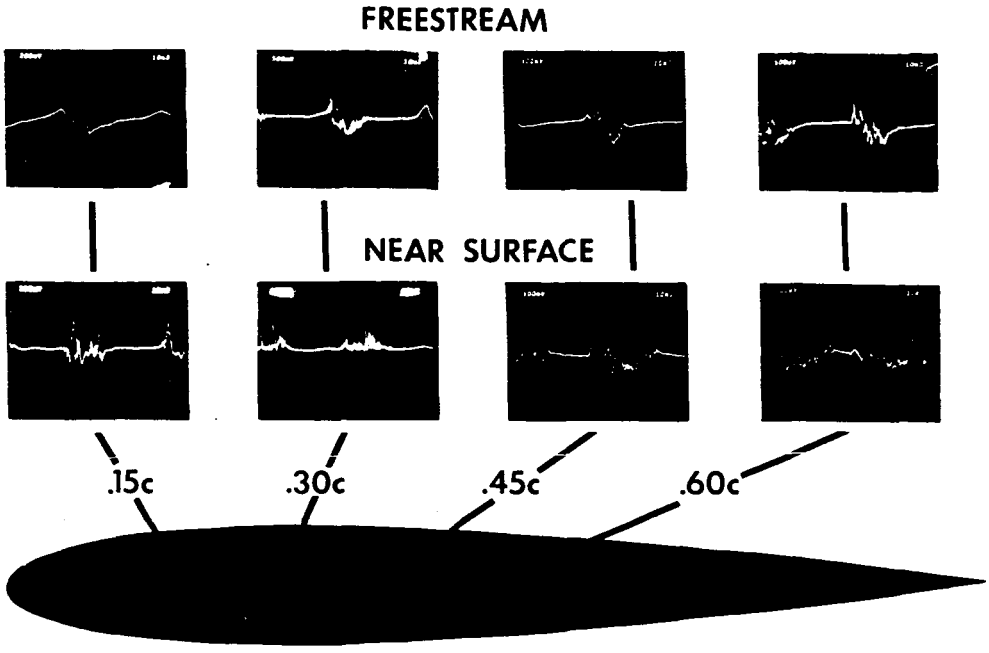

Figure 9. Time-dependent crossflow velocities measured in the propeller slipstream.

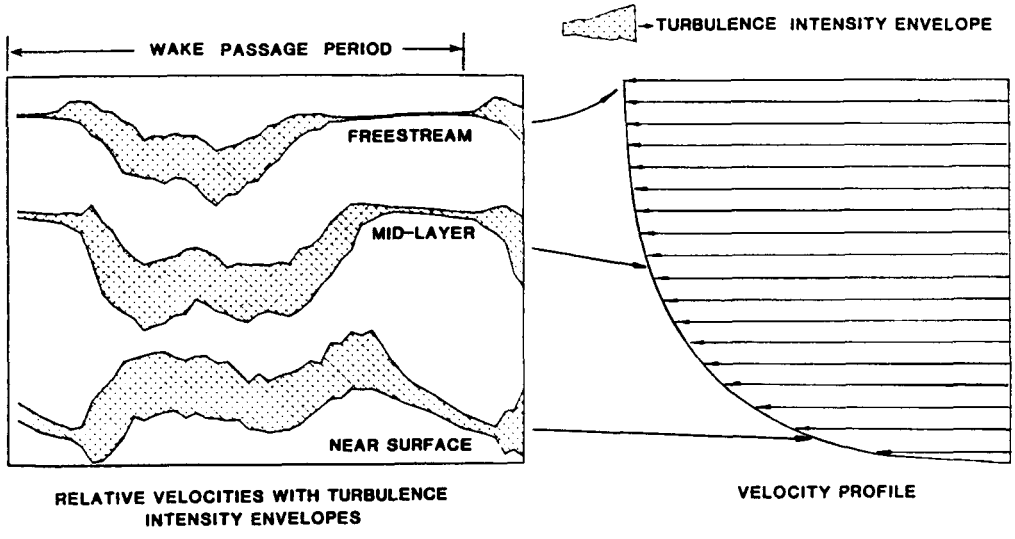

Figure 10. Representative time-dependent turbulence intensity measurements across a propeller blade wake passage cycle.

Boundary Layer Profile Measurement Results - The data recorded in the second series of experiments consisted of velocity time histories at different heights above the surface within the boundary layer. Sufficient data were taken to construct time histories of the mean velocity profile, and of the turbulence intensity at each corresponding point within the profile. A representative plot of these data is given in Figure 10. The mean streamwise velocity across a blade wake passage cycle is plotted with the turbulence intensity superimposed as a "turbulence intensity envelope". Three positions across the boundary layer are displayed. The upper trace shows the external flow turbulent disturbance. There is a velocity defect, characteristic of momentum-loss wake profiles. The middle trace shows the growth of the turbulence as one proceeds into the boundary layer. The lower trace shows the response near the surface to be an increase to a turbulent velocity followed by a decay back to the laminar state, as has been seen previously. The turbulence intensity decreases with the reversion to laminar flow.

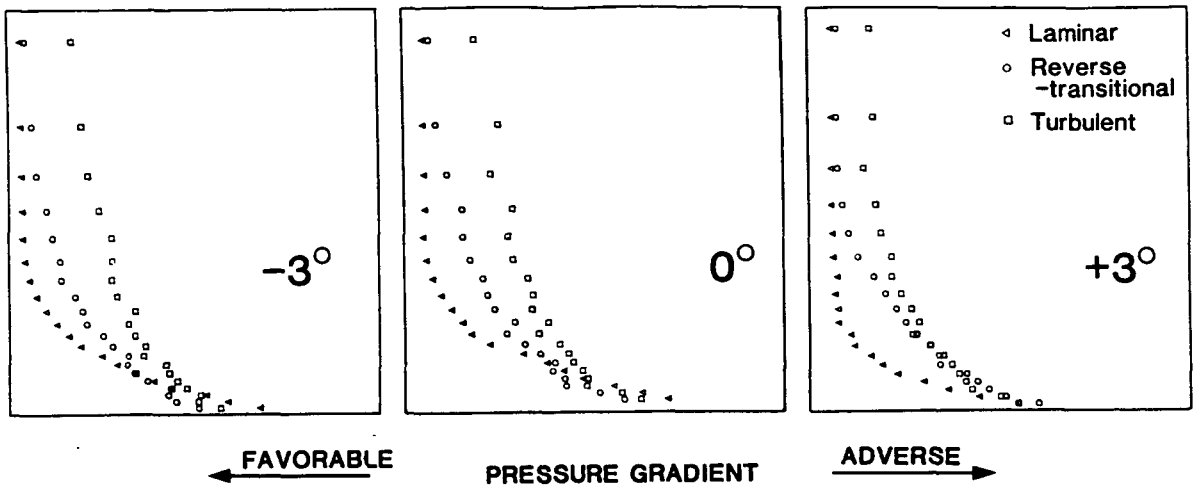

Figure 11. Boundary layer profiles at 45 percent chord location at three angles of attack for three time positions in blade wake passage cycle.

Figure 11 shows three sets of velocity profiles, each set including three profiles at different points in the cycle. Each set represents a different angle of attack, giving pressure gradient effects ranging from favorable to adverse. The profiles were not normalized with respect to their individual thicknesses, so their respective true thicknesses are reflected in the figure. Without the usual thickness normalization, the laminar profile appears to be fuller relative to the turbulent profiles. Applying the normalization would show the turbulent profile to be fuller, as is well established by theory. Note that the bottom line does not represent the surface of the airfoil but the lowest point in the boundary layer at which measurements could be taken.

The laminar profile is easily recognizable by the linear velocity gradient near the surface. The turbulent profile displays a greater thickness than the laminar as well as a higher velocity near the surface. The third profile shape to be noted starts at the external flow with a higher velocity than the fully turbulent, and returns to a more turbulent profile as the mid-layer is reached. This third profile lies in the reverse-transitional part of the cycle where the flow is reverting to the laminar state. This is best noted in the the case of the adverse pressure gradient at +3 degrees angle of attack. These time-dependent profile measurements help clarify the peculiar time-averaged profiles measured by Holmes et al. (8) on the Bellanca Skyrocket in flight.

A second way to characterize the reverse-transitional behavior is to consider the level of turbulence intensity through the boundary layer. Referring to Figure 10, a vertical scan indicates that at the return to the laminar state in the external flow, there is a high level of turbulence intensity near the airfoil surface. In Figure 12 a velocity profile is plotted on the right with a turbulence intensity envelope superimposed. The increase in turbulence intensity is evident as one moves from the external flow towards the surface. Again, the bottom line represents the lower limit of measurement, and not the airfoil surface. It would be expected that the level of turbulence intensity would go to zero as the actual surface is approached. The graph on the left is the value of the turbulence intensity used to construct the envelope on the right.

A comparison with the turbulence intensity across the turbulent profile is shown in Figure 13. It can be seen that the level of turbulence intensity remains approximately constant at 14 percent (open squares) as opposed to the gradual increase to a level of 9 percent (solid circles) for the reverse-transitional case as the airfoil surface is approached. Experiments by Dyban, Epik and Surpun (10) show similar behavior for low and high levels of external flow turbulence. Results from their work are reproduced in Figure 13. Higher levels of external flow turbulence produce a constant level throughout the the boundary layer due to the controlling mechanism of penetration of the turbulence.

ORIGINAL PAGE IS
OF POOR QUALITY

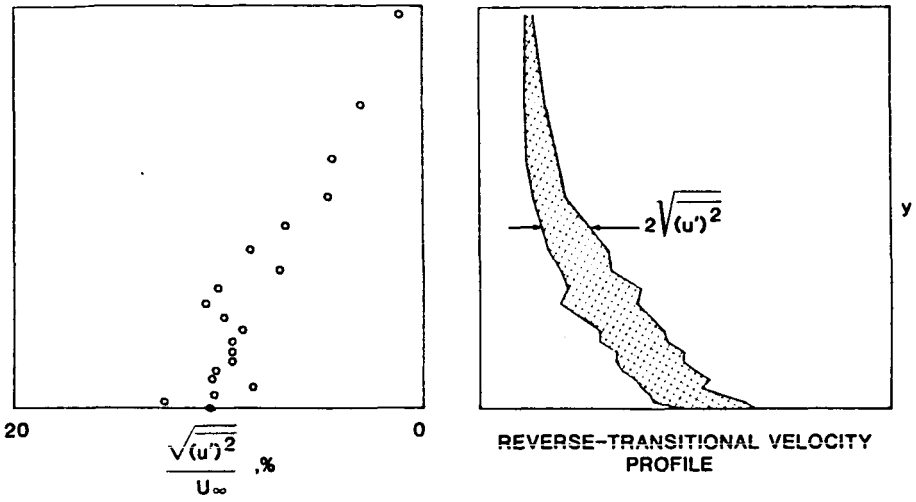

Figure 12. Turbulence intensity across the boundary layer for the reverse-transitional profile.

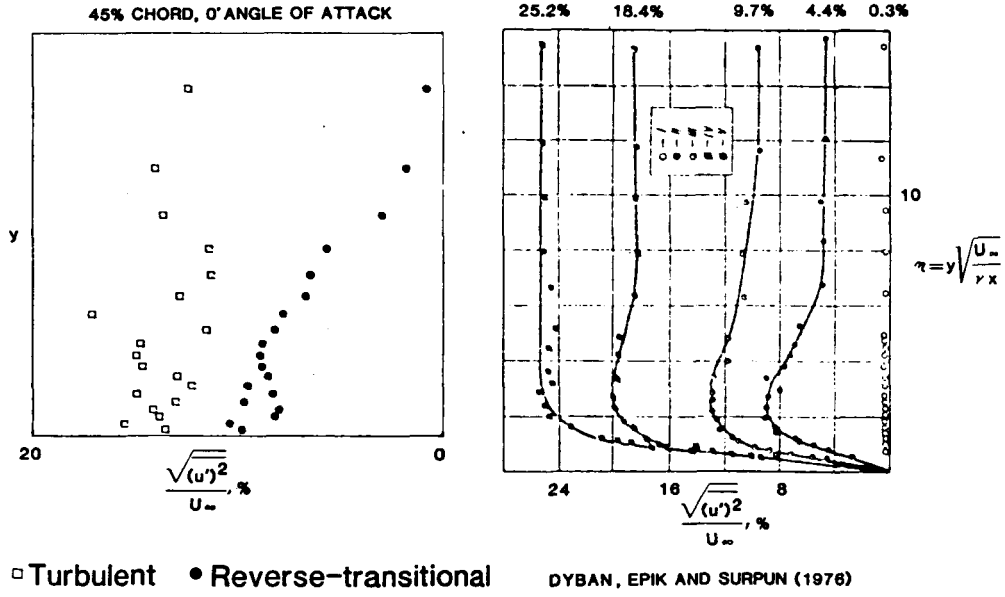

Figure 13. Comparison of turbulence intensities for two profiles with results of Dyban, Epik and Surpun (10).

On the other hand, lower levels of turbulence (on the order of a few percent) result in higher levels near the surface due to the mechanism of generation. Thus across a propeller blade wake passage cycle, the boundary layer at a point on the airfoil surface goes through the distinct phases of turbulent, reverse-transitional and laminar behavior consistent with a cyclic variation in external flow turbulence. An improved physical model can be proposed based upon the above observations, as shown in Figure 14. The model locally describes the shape of the mean velocity profile and the level of turbulence intensity across the boundary layer.

ANALYTICAL MODELLING

The Cebeci-Carr boundary-layer code (11) was used in a preliminary attempt to numerically model the boundary layer response to the propeller slipstream. Computer runs were made for the simple case of flat plate flow in which the turbulent solution procedure was switchedon, then switched off back to the laminar solution procedure. Switching-on of the turbulent solution procedure is what normally occurs in a boundary layer analysis code after the transition criteria have been satisfied at some point in the flow. For the Cebeci-Carr code, this was relatively

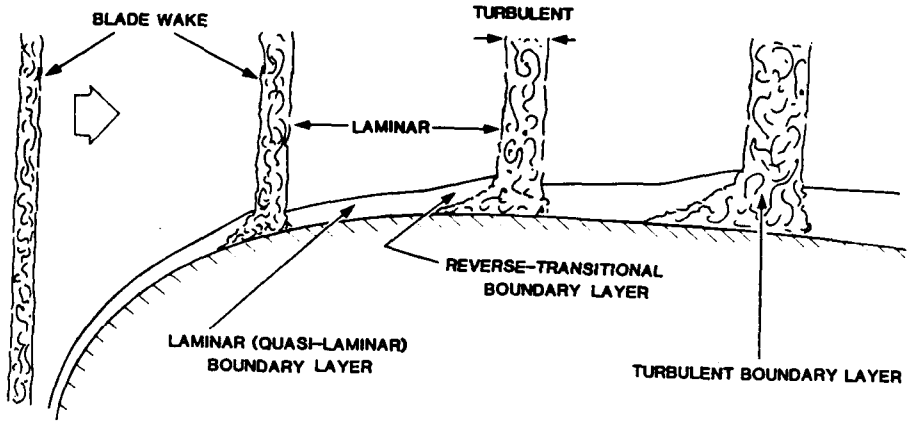

Figure 14. Propeller slipstream disturbance flow model showing turbulent response in boundary layer.

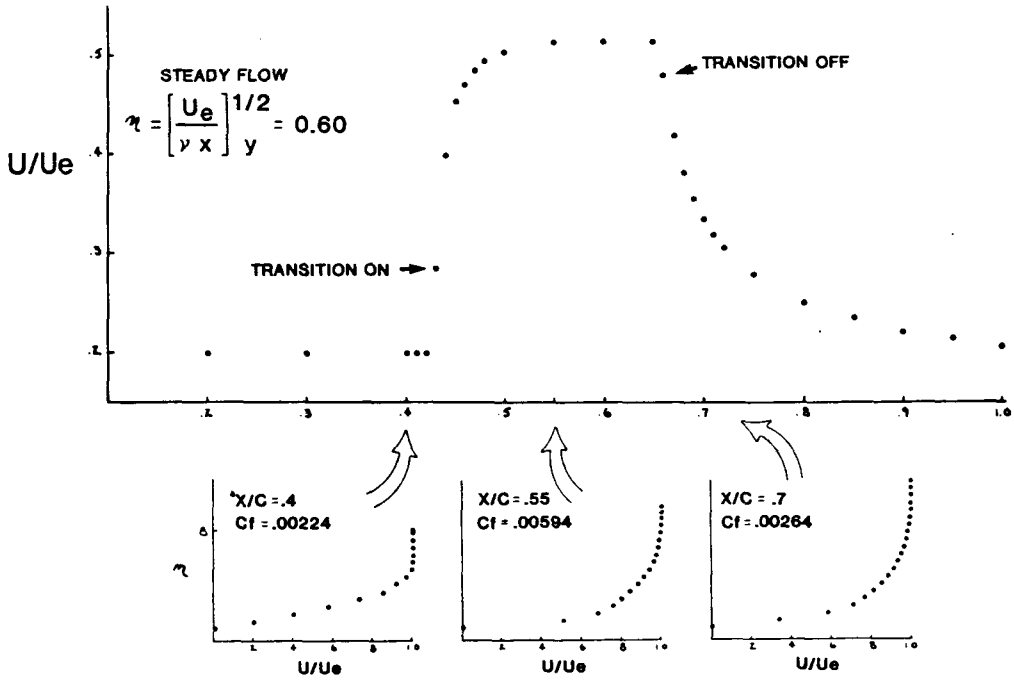

Figure 15. Numerical modelling of laminar/turbulent/-reverse-transitional cycle in boundary layer for flat plate flow.

easy to accomplish as the only difference in the solution procedures was the inclusion of an eddy viscosity model for the turbulent part. An attempt was made to model the reverse-transitional region observed experimentally by switching back to the laminar solution. Figure 15 shows the results for a representative case. The velocity ratio plotted in the top graph is the calculated value corresponding to a point approximately the same height above the surface as the experimental measurements. The sharp rise in velocity, the steady turbulent level, and the laminar decay observed experimentally (see Figure 8) can be seen in this solution procedure. The cause of this behavior can be ascertained in the lower part of the figure by noting the change of profile shape from laminar, to turbulent, to reverse-transitional.

ORIGINAL PAGE IS
OF POOR QUALITY

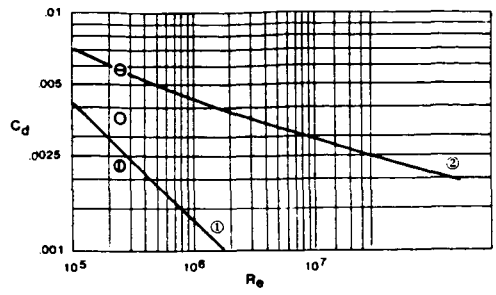

DRAG COEFFICIENT FOR FLAT PLATE FLOW

① Laminar theory, from Blasius
② Turbulent theory, from Prandtl-Schlichting
① Laminar, using Cebeci-Carr Cd=.0024
O Mixed laminar/turbulent, Cebeci-Carr Cd=.0038
⊖ Turbulent, Cebeci-Carr Cd=.0058

Figure 16. Comparison of calculated cyclic mixed laminar/turbulent drag coefficient with fully laminar and fully turbulent solutions.

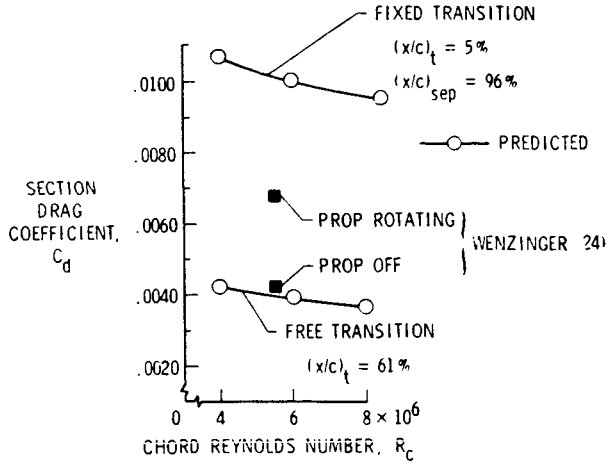

Figure 17. Comparison of measured drag (solid squares) with and without slipstream, with calculated drag (open circles).

By performing this procedure multiple times across the flat plate and integrating the skin friction values, a sectional drag coefficient was determined. This drag coefficient, and the values calculated by the Cebeci-Carr program for the fully laminar and fully turbulent cases are given in Figure 16, along with the well known Blasius and Prandtl-Schlichting curves. The cyclic laminar/turbulent drag coefficient lies between the fully laminar and fully turbulent values as might be expected. This result agrees with calculations performed by Holmes, et al. (7) in regards to an early wind tunnel investigation reported by Wenzinger (12). Wenzinger made wake survey drag measurements of a powered wind tunnel model wing with propeller running and propeller off. Utilizing the Eppler airfoil design and analysis code (13), Holmes demonstrated that the propeller-on drag value lies between the normal free transition case and the fully turbulent case. Referring to Figure 17, the wing section drag coefficient with slipstream is only 60 percent greater then the value obtained if the full possible extent of laminar flow were realized. On the other hand, if the wing boundary layer is fully turbulent, the drag increase is 150 percent above laminar. It should be noted in Figure 17, that the free transition calculation agrees with the propeller-off drag measurement. The drag reduction benefits of NLF design philosophy extend into the slipstream region also.

Two independent and different analytical investigations coupled with experimental measurements lead to the same general conclusion: the effect of the propeller slipstream on the wing boun dary layer is to increase the drag coefficient above the free transition value, but not to the extent of a fully turbulent value as early investigations suggested.

The results of the analytical investigations suggest that a practical boundary layer analysis procedure can be formulated to predict wing section drag within a slipstream. As a better understanding of the boundary layer behavior in a slipstream is developed, certain characteristics may emerge which could be useful in the design of wing sections for this flow region.

CONCLUSIONS

A cyclic laminar and turbulent flow has been observed in the wing boundary layer in the propeller slipstream. The flow displays a coherent behavior which may be modelled numerically.

Boundary layer measurements indicate the existence of three types of velocity profiles that characterize the time-dependent flow: turbulent, reverse-transitional and laminar. The type of profile has been further characterized by the turbulence intensity level throughout the boundary layer.

With these results, an improved physical model of the boundary layer in the propeller slipstream is proposed. A greater understanding of the physics of the flow in the slipstream and an accurate computational method of predicting the boundary layer behavior there may lead to the design of NLF airfoils tailored for those conditions.

Drag reduction benefits can be obtained by applying NLF design philosophy to airframe surfaces within the slipstream.

Tractor propeller installations should not be automatically excluded from NLF aircraft design.

ACKNOWLEDGEMENT

This work is supported by NASA Langley Research Center Grant NAG 1-344. The technical monitor is Dr. Bruce J. Holmes.

REFERENCES

(1) Miley, S.J. and von Lavante, E.: "Propeller Propulsion System Integration - State of Technology Survey," NASA CR-3882, July 1984.

(2) Young, A.D. and Morris, D.E.: "Note on Flight Tests on the Effect of Slipstream on Boundary Layer Flow," R&M No. 1957, Brit. A.R.C., 1939.

(3) Young, A.D. and Morris, D.E.: "Further Note on Flight Tests on the Effect of Slipstream on Boundary-Layer Flow," RAE Rep. No. B.A. 1404b, 1939.

(4) Hood, M.J. and Gaydos, M.E.: "Effects of Propellers and Vibration on the Extent of Laminar Flow on the NACA 27-212 Airfoil," NACA ACR (WR L-784), 1939.

(5) Zalovcik, J.A.: Flight Investigation of the Boundary Layer and Profile Drag Characteristics of Smooth Wing Sections on a P-47D Airplane," NACA WR L-86, 1945.

(6) Zalovcik, J.A., and Skoog, R.B.: Flight Investigation of Boundary Layer Transition and Profile Drag of an Experimental Low-Drag Wing Installed on a Fighter-Type Airplane," NACA WR L-94, 1945.

(7) Holmes, B.J.; Obara, C.J.; and Yip, L.P.: "Natural Laminar Flow Experiments on Modern Airplane Surfaces," NASA TP 2256, 1984.

(8) Holmes, B.J., Obara, C.J., Gregorek, G.M., Hoffman, M.J., and Freuhler, R.J.: "Flight Investigation of Natural Laminar Flow on the Bellanca Skyrocket II," SAE Paper 830717, 1983.

(9) Sparks, S.P. and Miley, S.J.: "Development of a Propeller Afterbody Analysis with Contracting Slipstream," SAE Technical Paper Series 830743, April 1983.

(10) Dyban, Ye.P., Epik, E.Ya., and Surpun, T.T.: "Characteristics of the Laminar Boundary Layer in the Presence of Elevated Free-Stream Turbulence," Fluid Mechanics - Soviet Research, Vol. 5, No. 4, July-August 1976, pp. 30-36.

(11) Cebeci, T. and Carr, L.W.: "A Computer Program for Calculating Laminar and Turbulent Boundary Layers for Two-Dimensional Time-Dependent Flows," NASA TM-78470, March 1978.

(12) Wenzinger, C.J.: "Wind Tunnel Investigation of Several Factors Affecting the Performance of a High Speed Pursuit Airplane with Air-Cooled Engine," NACA ACR, Nov. 1941 (Available as 82-N74537).

(13) Eppler, R. and Somers, D.M.: "A Computer Program for the Design and Analysis of Low Speed Airfoils," NASA TM-80210, 1980.

PROPELLER SLIPSTREAM/WING BOUNDARY LAYER EFFECTS AT LOW REYNOLDS NUMBERS

Stan J. Miley and Richard M. Howard
Department of Aerospace Engineering
Texas A&M University
College Station, Texas 77843

Bruce J. Holmes
NASA Langley Research Center
Hampton, Virginia 23665

ABSTRACT

The effects of a propeller slipstream on the wing laminar boundary are being investigated. Hot-wire velocity sensor measurements have been performed in flight and in a wind tunnel. It is shown that the boundary layer cycles between a laminar state and a turbulent state at the propeller blade passage rate. The cyclic length of the turbulent state increases with decreasing laminar stability. Analyses of the time varying velocity profiles show the turbulent state to lie in a transition region between fully laminar and fully turbulent. The observed cyclic boundary layer has characteristics similar to relaminarizing flow and laminar flow with external turbulence.

INTRODUCTION

A research program is in progress to investigate the behavior of the laminar boundary layer as affected by a propeller slipstream. Although the investigation is directed towards manned propeller driven aircraft, much of the experimental work to date has been performed at Reynolds numbers less than 1×10^6. These results are therefore also applicable to low Reynolds number aircraft.

Early observations of the effect of the propeller slipstream on boundary layer transition have not resulted in consistent conclusions. Young and Morris [1,2], and Hood and Gaydos [3] concluded from their investigations that the propeller slipstream caused the point of transition to move forward to a location near the leading edge. Reports by Zalovcik [4], and Zalovcik and Skoog [5] describe wing boundary layer measurements in propeller slipstreams performed on P-47 aircraft utilizing an NACA 230 series wing section and an NACA 66 series laminar flow wing section. Their results show little effect of the slipstream on transition for the NACA 230 section; however, the test with the NACA 66 series section resulted in the transition point location moving forward from 50 to 20 percent chord. The general consensus from this early work is that the propeller slipstream reduced the extent of laminar flow by forcing transition to occur earlier.

Recent work by Holmes, Obara and Yip [6] and Holmes, et al. [7] brings into question the validity of the ability of the early

measurement methods to accurately determine transition. Time-dependent behavior, particularly at frequencies associated with propeller blade passage rate, was not measurable by techniques commonly employed at that time. Measurements by Holmes, et al. [7] using surface hot-wire sensors indicate the existence of a cyclic turbulent behavior resulting in convected regions of turbulent packets between which the boundary layer appears to remain laminar (Figure 1).

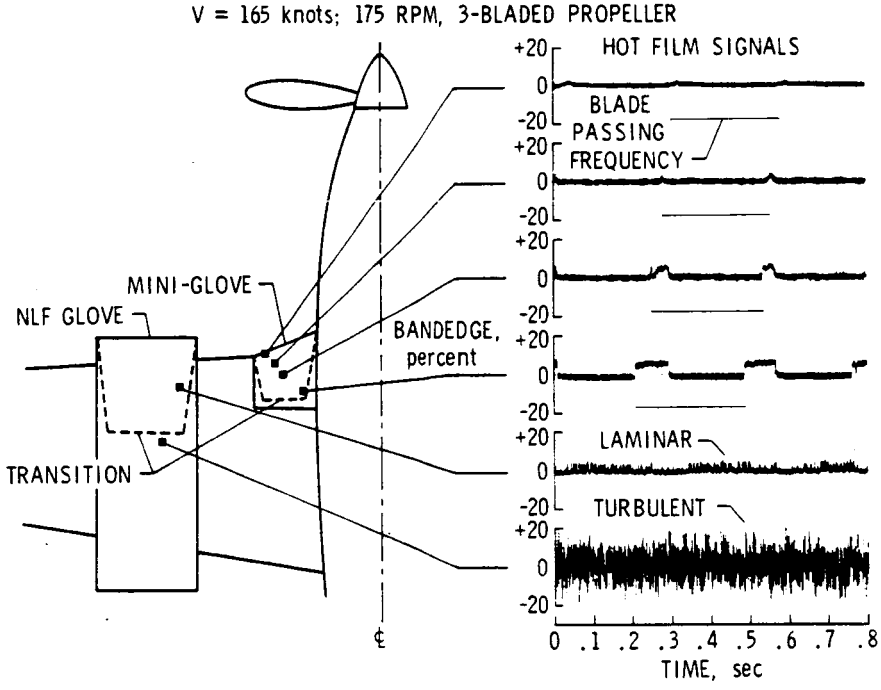

Figure 1. Surface hot-film measurements by Holmes et al. [7] showing cyclic laminar/turbulence behavior of boundary layer within propeller slipstream.

EXPERIMENTAL INVESTIGATIONS

Flight Experiments

At Texas A&M University, flight measurements of the wing boundary layer in the slipstream have been made on a Gulfstream Aerospace GA-7 Cougar at two chord locations using a dual-probe hot-wire velocity sensing system. One probe was located adjacent to the surface well within the boundary layer and the other was located directly above in the external flow. The results of the flight test are shown in Figures 2-4.

The signal traces are time histories of the local flow velocities in the boundary layer near the surface and in the external flow. The boundary layer velocity signal shows a periodic laminar/turbulent behavior. The change to turbulent flow results in an increase in the velocity seen by the probe because of the fuller turbulent profile. This change in profile results from periodic disturbances in the external flow due to the viscous wake shed from the propeller blade.

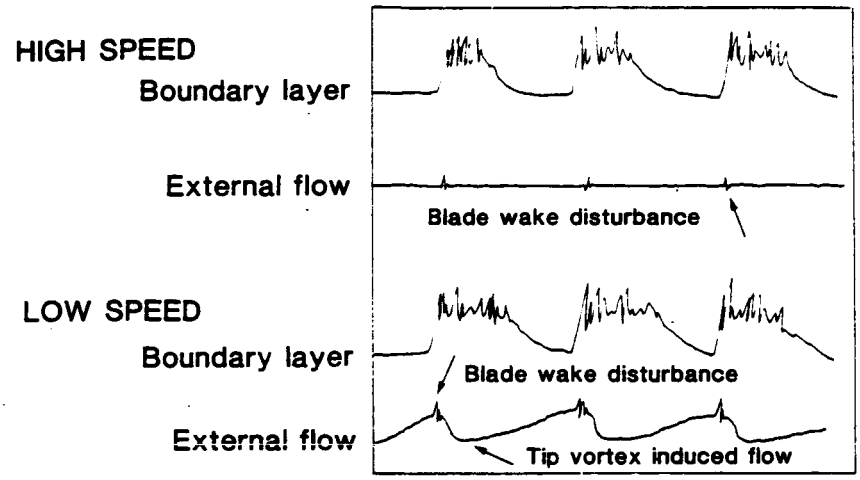

Figure 2. Identification of hot-wire velocity sensor signals in Figures 3-4.

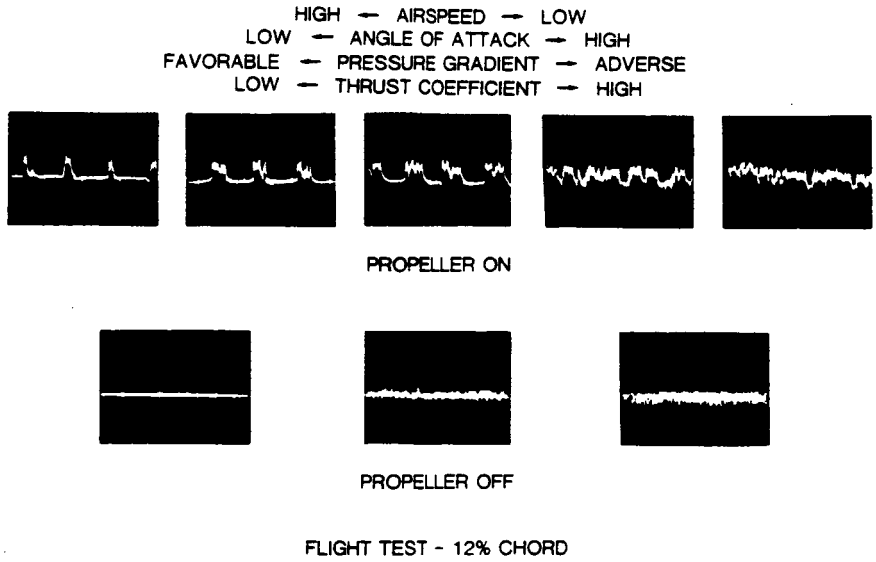

Figure 3. Velocity signal in boundary layer near surface, showing cyclic laminar/turbulent flow (propeller on) and laminar-transition- turbulence (propeller off).

The length of time which the cyclic turbulence remains in the boundary layer is dependent upon the laminar stability in the differing pressure gradients from the high-speed to the low-speed end. At the high-speed end, the pressure gradient is strongly favorable, and laminar stability is correspondingly high. Here, the boundary layer reverts almost immediately back to laminar flow after the passage of the external disturbance. At the low-speed end, the pressure gradient is no longer strongly favorable, laminar stability is greatly decreased, and the turbulence remains for almost the total cycle.

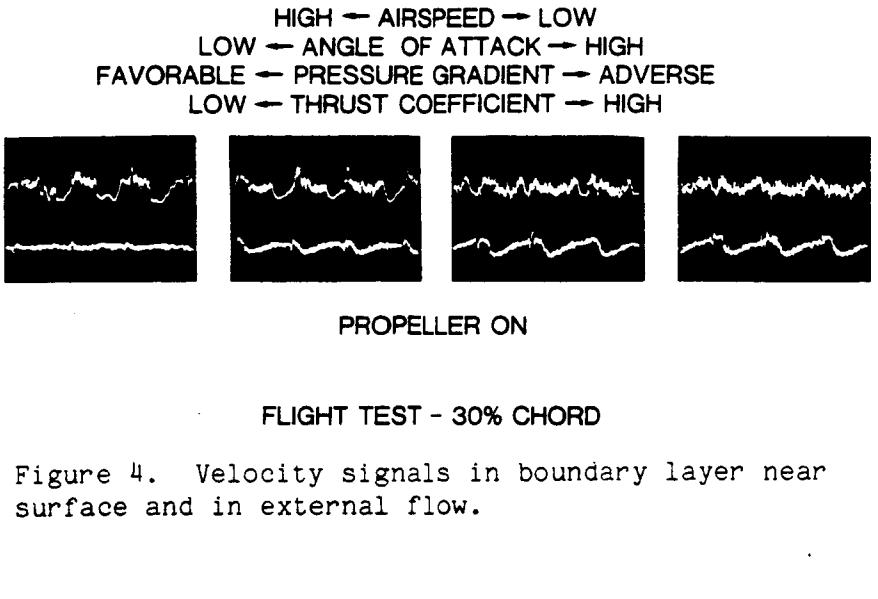

Figure 4. Velocity signals in boundary layer near surface and in external flow.

The effect of reduced laminar stability at the 30 percent chord location is evident in Figure 4. Here also is seen the character of the external flow disturbance due to the propeller slipstream. The viscous blade wake appears as a short wave impulse barely discernible at the high-speed end. As the speed is reduced, the propeller blade operates at an increasingly higher angle of attack and the viscous wake grows, leading to a more pronounced impulse disturbance signal. This is noted in the figures in terms of the propeller thrust coefficient. The low frequency wave pattern which develops in the external slipstream flow is due to the propeller tip vortex. As demonstrated by Sparks and Miley [8], the helical tip vortex induces an axial component in the slipstream velocity which increases with vortex strength (propeller thrust coefficient), and as the edge of the slipstream boundary is approached. While the tip vortex induced flow dominates the slipstream velocity signal, it will be shown that it is the relatively smaller blade viscous wake disturbance which is affecting the laminar boundary layer.

A slipstream disturbance flow model (Figure 5) was constructed from an analysis of the flight data. The viscous wake from the propeller blade forms a helical sheet which is split by the wing. The turbulence in the helical wake is seen by a stationary point in the boundary layer as a periodic change in external flow turbulence. The laminar boundary layer responds by transitioning to the turbulent state and then returning to the laminar state through a reverse-transitional process based upon the degree of local laminar stability.

Wind Tunnel Investigation

A small-scale wind tunnel test program was begun to study the boundary layer response in more detail. The test model was a 30-inch chord NACA 0012 composite wing section with an 18-inch diameter single-bladed propeller and electric motor mounted at wing level at

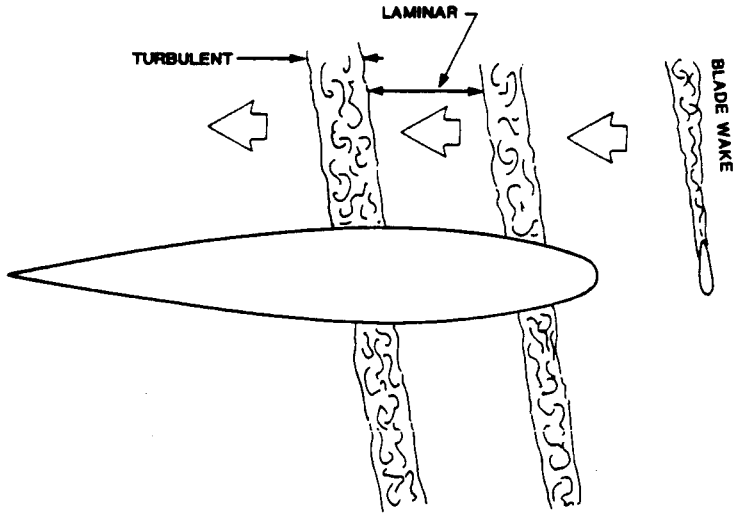

Figure 5. Slipstream disturbance flow model.

one-fifth chord distance upstream. Measurements were made at various angles of attack with a constant temperature hot-wire anemometer system and dual-probe configuration similar to that used in flight. The probes were traversed in a chordwise direction along the airfoil with the probe support free to pivot allowing the sensors to follow the airfoil contour. The probe heights above the surface were maintained at approximately 0.01 and 1.0 inches.

Two runs are shown in Figures 6-8. Figure 6 describes the signals seen in the photographs in the following figures. In each photograph the upper trace is the velocity in the boundary layer near the surface; the middle trace is the velocity for the external flow probe; and the lower trace is the trigger signal for the oscilloscope obtained from a magnetic proximity transducer sensing propeller blade passage. Figure 7 shows a series of measurements at -3 degrees angle of attack resulting in a favorable pressure gradient along the upper surface. The upper row of photographs shows time histories of velocities at chord locations indicated with the propeller off. Transition takes place at approximately 70 percent chord at a chord Reynolds number of 6×10^5. Low frequency Tollmien-Schlichting waves appear with intermittent bursts of turbulence.

The lower row of photographs shows the velocities measured with the propeller running. The growth of the turbulent part of the cycle increases with decreasing laminar stability in the chordwise direction. Evident also is cyclic relaminarization of the previously turbulent region on the aft portion of the airfoil. Note this effect in the photograph for the 80 percent chord location. This behavior was seen in the flight data, but is more pronounced here, possibly due to the low Reynolds number. The waveform of the cyclic velocity variation can be noted, with the immediate jump to a turbulent velocity level with the arrival of the external disturbance. After the disturbance passes, the velocity returns to the laminar level as an exponential decay.

ORIGINAL PAGE IS
OF POOR QUALITY

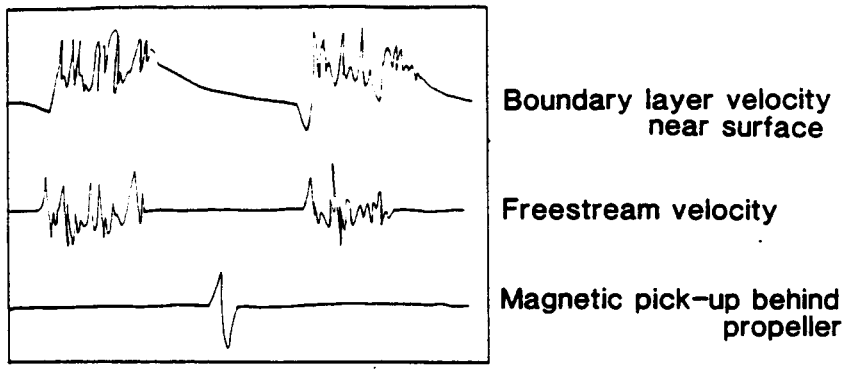

Figure 6. Identification of hot-wire velocity sensor signals in Figures 7-8.

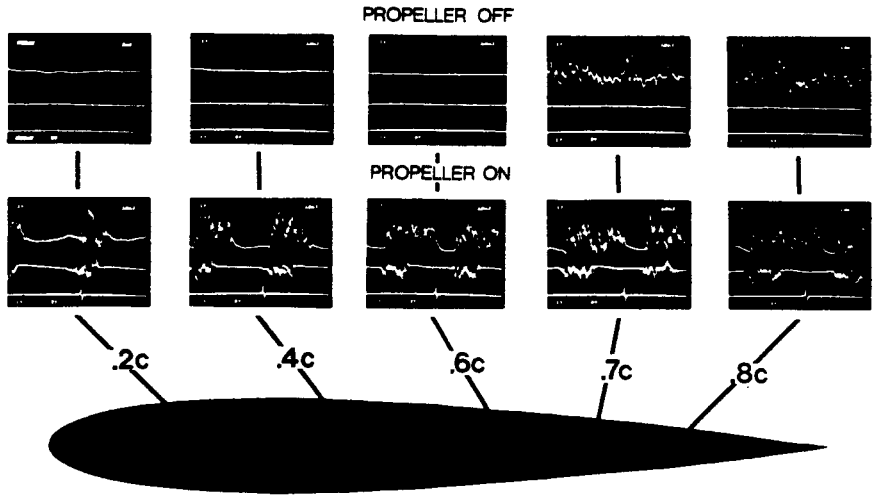

Figure 7. Velocity signals in boundary layer near surface and in external flow, showing cyclic laminar/turbulent flow (propeller on) and laminar-transition-turbulence (propeller off). -3° angle of attack.

Figure 8 shows the results for 1 degree angle of attack. The pressure gradient is less favorable over the upper surface; the laminar boundary layer responds by transitioning now at 40 percent chord. More evident here is the cyclic relaminarization of the previously turbulent boundary layer. For the low test Reynolds number, the propeller slipstream appears to have a beneficial effect in the turbulent flow region of the airfoil. The mechanism behind the relaminarization is not understood at present. Possibilities include a reaction to the cyclic external flow turbulence and/or three-dimensional effects from the swirl component in the helical wake sheet.

ORIGINAL PAGE IS
OF POOR QUALITY

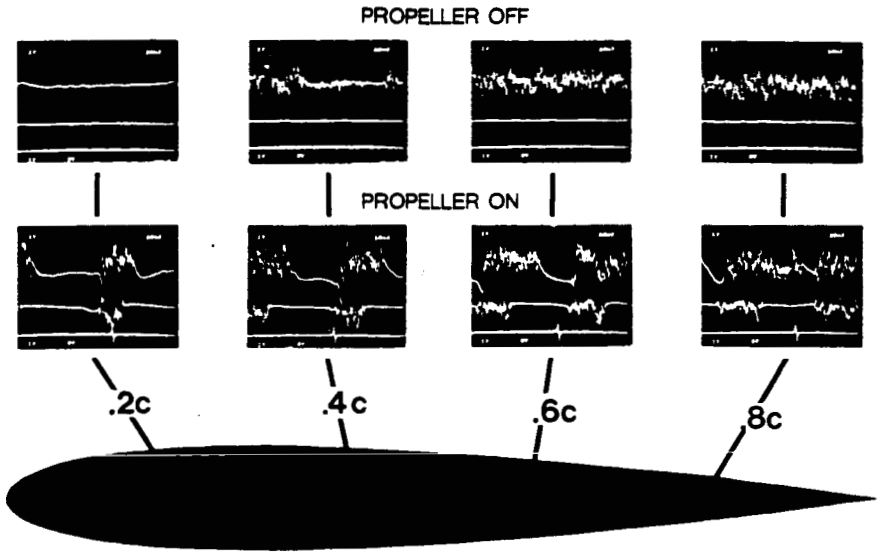

Figure 8. Velocity signals in boundary layer near surface and in external flow, showing cyclic laminar/turbulent flow (propeller on) and laminar-transition-turbulence (propeller off). +1° angle of attack.

A second series of experiments was conducted utilizing a single hot-wire probe to traverse the boundary layer normal to the surface. Runs were made at three angles of attack. The velocity time histories were digitized through a microcomputer and stored on floppy disk for analysis. Sufficient data were taken to construct time histories of the mean velocity profile, and of the turbulence intensity at each corresponding point within the profile. A representative plot of these data is given in Figure 9. The mean streamwise velocity across a blade wake passage cycle is plotted with the turbulence intensity superimposed as a "turbulence intensity envelope". Three positions across the boundary layer are displayed. The upper trace shows the external flow turbulent disturbance. There is a velocity defect, characteristic of momentum-loss wake profiles. The lower trace shows the response near the surface to be an increase to a turbulent velocity followed by a decay back to the laminar state, as has been seen previously. The turbulence intensity decreases with the reversion to laminar flow.

ANALYSIS AND RESULTS

Figure 10 shows three sets of velocity profiles, each set including three profiles at different points in the wake passage cycle. Each set represents a different angle of attack, giving pressure gradient effects ranging from favorable to adverse. The profiles were not normalized with respect to their individual thicknesses. Note that the bottom line does not represent the surface of the airfoil but the lowest point in the boundary layer at which measurements could be taken. The profiles within each set are identified according to their position in the wake passage cycle, i.e. "laminar," "reverse-transitional," and "turbulent". Each of these positions also

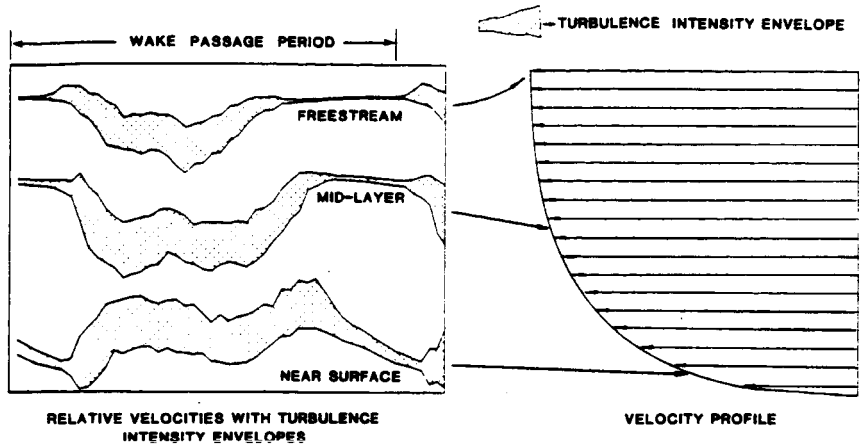

Figure 9. Time histories of the mean velocity and turbulence intensity at three vertical positions in the boundary layer. Data for one wake passage cycle.

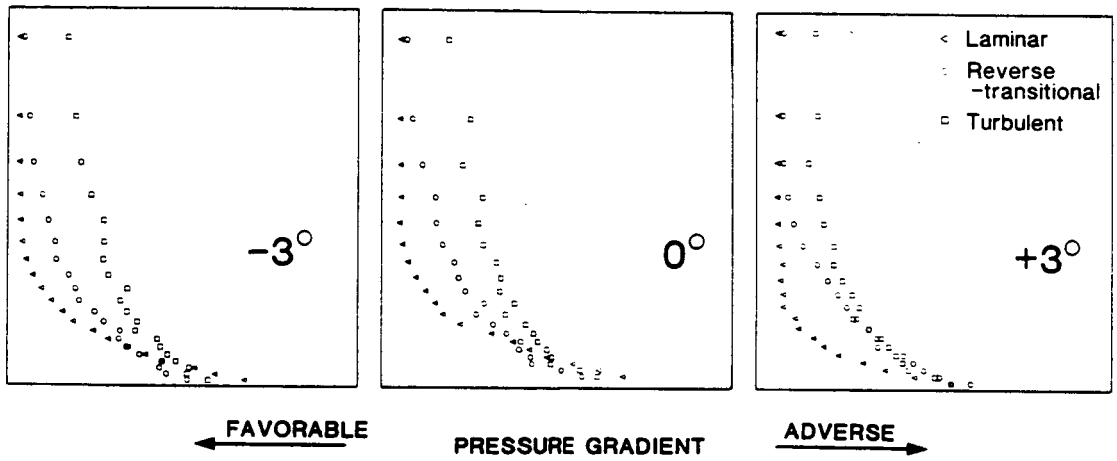

Figure 10. Boundary layer velocity profiles for three different angles of attack and for three different positions in the wake passage cycle.

corresponds to a level of external flow turbulence intensity. The turbulence intensity distribution (profile) through the boundary layer for the 0 degree angle of attack case is shown in Figure 11. Due to limitations of the digitizer, the upper cut-off frequency of the data is approximately 100 hertz. Also, the wind tunnel has a low frequency unsteadiness which was not removed from the data. It is seen that there is a correspondence between the external flow turbulence intensity, the boundary layer velocity profile, and the boundary layer turbulence intensity profile.

The effect of external flow turbulence on laminar and turbulent boundary layers has been investigated to a limited extent, primarily with concern to heat transfer. The work of Dyban, Epik and Surpun [9] is summarized in Figure 12. The laminar boundary layer over a flat

ORIGINAL PAGE IS
OF POOR QUALITY

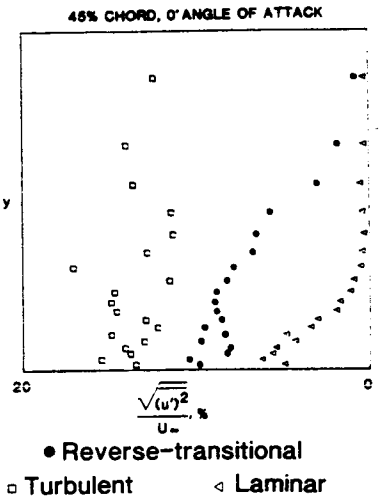

Figure 11. Turbulence intensity profiles for three different positions in the wake passage cycle. 0° angle of attack.

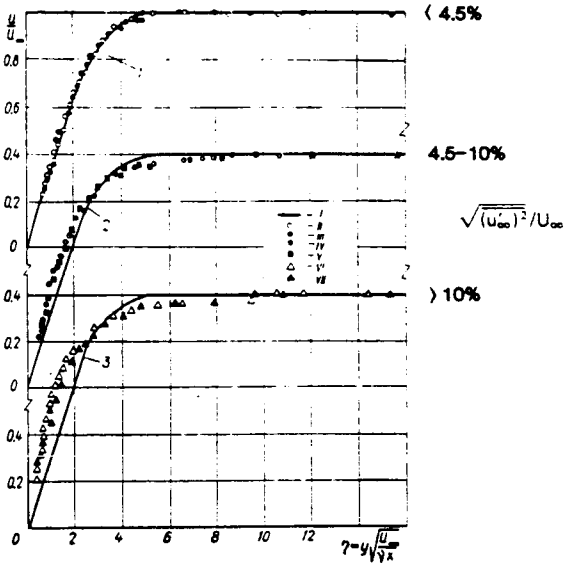

a) Boundary layer velocity profiles for three ranges of external flow turbulence. Blasius (flat plate) profile shown for reference.

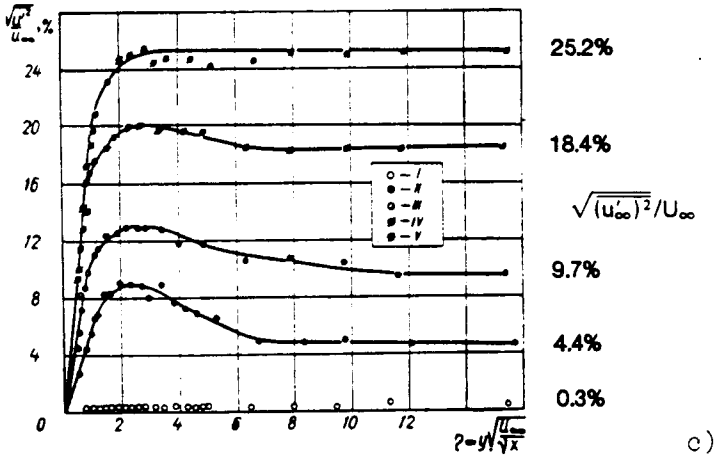

b) Boundary layer turbulence intensity profiles for different external flow turbulence intensity levels.

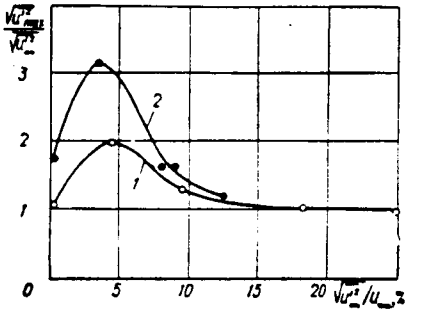

c) Ratio of boundary layer peak turbulence intensity to external flow turbulence intensity for two different Reynolds numbers.

Figure 12. Results from Dyban et al. [9].

plate is subjected to different levels of external flow turbulence intensity. The resulting boundary layer velocity and turbulence intensity profiles are shown in the figure. As the external flow turbulence intensity is increased, the velocity profile becomes fuller. Three distinct ranges of external turbulence intensity have been identified according to the respective generation of turbulence within the boundary layer. As shown in Figure 12c, these ranges are: for an external turbulence intensity less than 4.5 percent, the generated turbulence intensity in the boundary layer increases at a faster rate

than the external flow turbulence intensity, the generated intensity reaching peak levels 2 to 3 times as large depending on the Reynolds number; for 4.5 to 10 percent external flow turbulence intensity, the generated turbulence intensity in the boundary layer increases at a slower rate than the external flow turbulence intensity, reversing the trend in the first range; and for an external flow turbulence intensity greater than 10 percent, the rate of increase of generated turbulence intensity in the boundary layer monotonically approaches that of the external flow. The boundary layer velocity and turbulence intensity profiles in Figure 12 are identified respectively according to these ranges.

Comparison of the wind tunnel measurements with the the work of Dyban et al. [9] supports the view that the laminar boundary layer within the slipstream can be characterized as a boundary layer with a cyclic variation of external flow turbulence. As indicated in Figure 5, the source of the external flow turbulence is the viscous wake from the propeller blade. The passage of the wake over a point on the wing alters the laminar boundary layer according to the behavior shown in Figures 10-12. The increase in mean velocity shown in Figures 2-4 is the result of the change in the velocity profile. The length of the turbulence signal in Figures 2-4 is in part due to the change in the turbulence intensity profile. The available data show that near the surface, the turbulence will persist some time after the passage of the external turbulence. It is expected that the local pressure gradient will affect the rate of decay of the generated turbulence. This is presently being investigated. It is also important to note that with a definite turbulence profile within the boundary layer, a single point measurement by a hot-wire sensor can give misleading information. A thinner boundary layer would register a shorter turbulence time length than a thicker one because of the relative position of the sensor. With the present understanding, the model of Figure 5 has been updated, and the current model is shown in Figure 13. In this figure the relative thickness of the boundary layer and the persistence of the turbulence is emphasized.

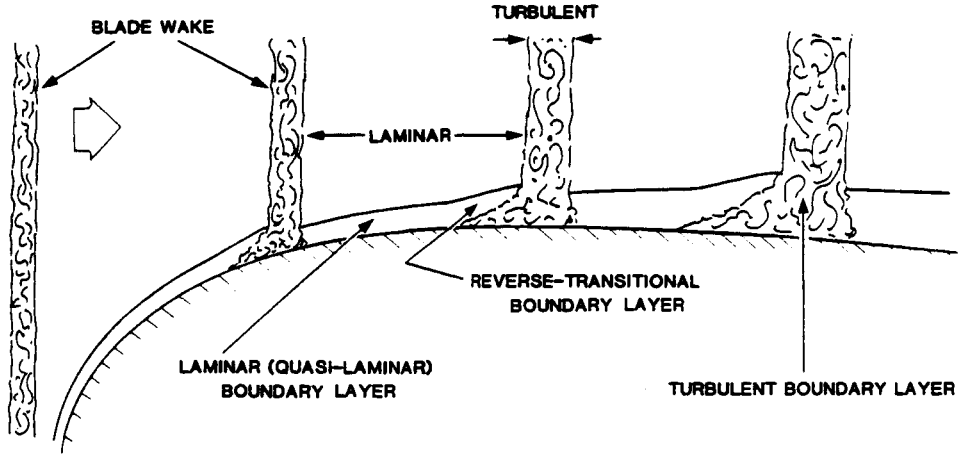

Figure 13. Current slipstream flow disturbance model, showing effect on laminar boundary layer.

An analysis was performed to determine where these external turbulence boundary layers lie in relation to conventional laminar and turbulent flows. Shape factor correlations between H_{12} and H_{32} were calculated from the wind tunnel data. Data for each time step in the wake passage cycle were averaged over fifty cycles, smoothed, fit with a cubic spline and integrated for values of H_{12} and H_{32}. Figure 14 shows the correlation across a wake passage cycle for an angle of attack of 0 degrees at chord locations of 15 and 45 percent, and for an angle of attack of 3 degrees at a chord location of 30 percent. Also included in the figure are the wake passage cycle time histories of the freestream mean velocity and turbulence intensity at the three chord positions. The curves plotted in the figure are the correlations utilized by Eppler [11] for laminar and turbulent flow as determined from similar solutions and empirical data.

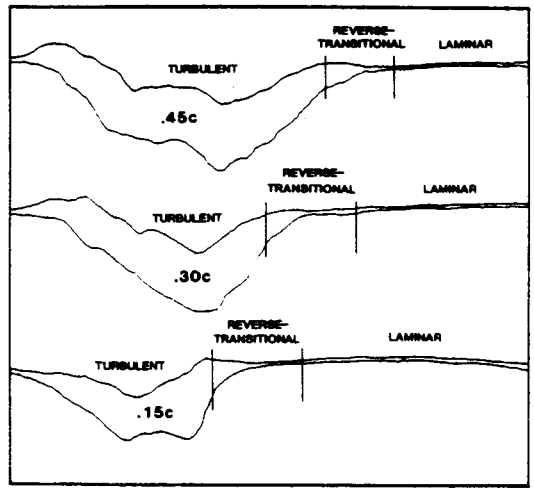

a) Time histories of external flow turbulence intensity.

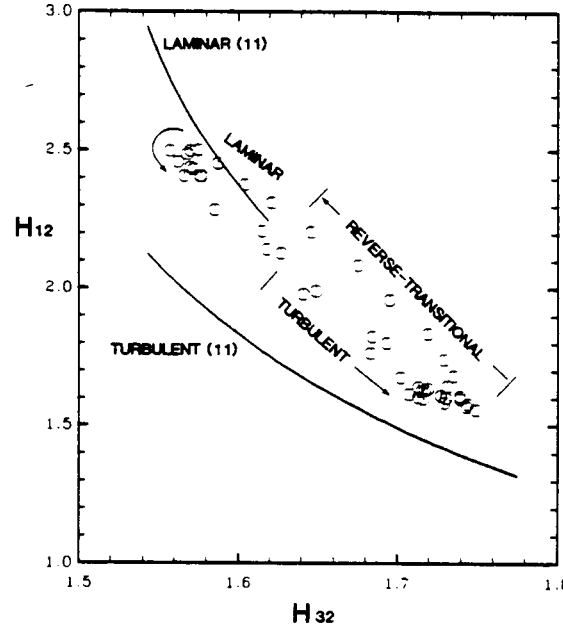

b) Shape factor variation for 15 percent chord. 0° angle of attack.

Figure 14. Variation of boundary layer shape factors through wake passage cycle.

In Figure 14 the time step data points corresponding to conditions where the boundary layer is indicated to be laminar lie on the laminar shape factor curve. The effect of the more adverse pressure gradient at 3 degrees angle of attack is seen by noting that the respective data points are shifted to lower vales of H_{32}. As the cycle is progressed, the velocity profile shifts to a highly stable form under the influence of the external turbulence, then reverts back to the conventional laminar range. In each case the shape factor correlation indicates that the boundary layer based on velocity profile behavior never attains the predicted turbulent relationship. In Figure 15, shape factors determined from the external turbulence flow boundary layer velocity profiles of Dyban et al. [9] and from relaminarization flow boundary layer velocity velocity profiles of reference [10] are plotted with the laminar and turbulent correlation curves. The external

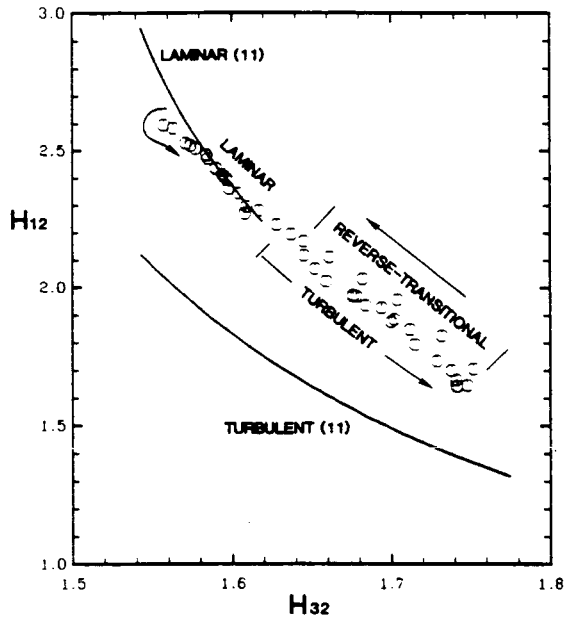

c) Shape factor variation for 45 percent chord. 0° angle of attack.

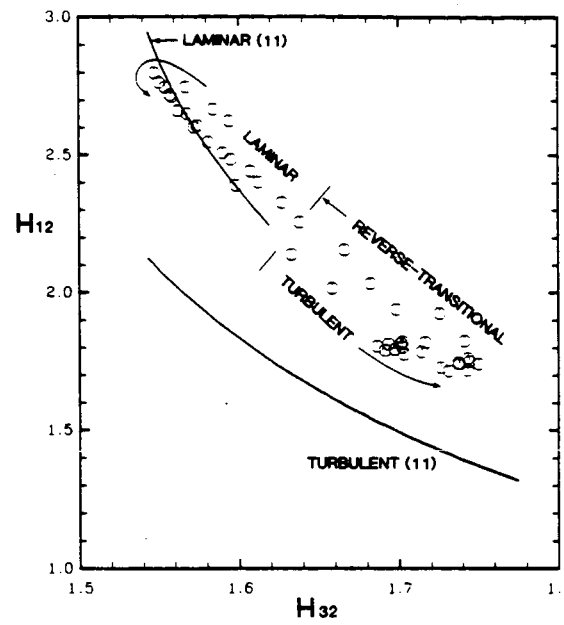

d) Shape factor variation for 30 percent chord. +3° angle of attack.

Figure 14. Concluded.

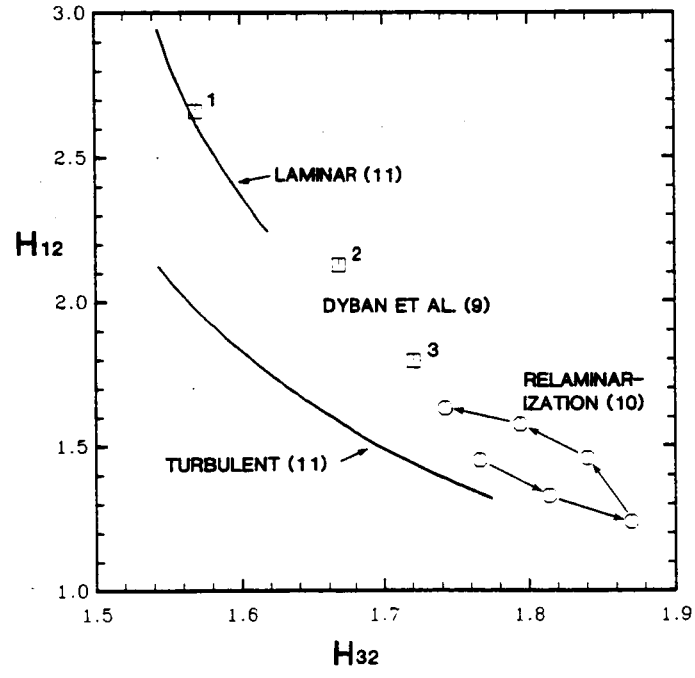

Figure 15. Boundary layer shape factor variation for external flow turbulence of Dyban et al. [9] and for relaminarizing flow [10].

turbulence shape parameter values follow that same path as the slipstream results. The relaminarizing flow shape parameter values initially move in the direction of a newer (younger) turbulent boundary layer, then loop back and proceed in the direction of the laminar curve. The relaminarizing boundary layer is initially turbulent. Under the action of a strongly favorable pressure gradient, a reversion to a laminar-like state takes place. The progress of the relaminarization in relation to the laminar and turbulent curves is noted in the figure. The turbulence intensity profiles of the relaminarizing flow from reference [10] are given in Figure 16. The profiles are similar to those of the external flow turbulence boundary layers.

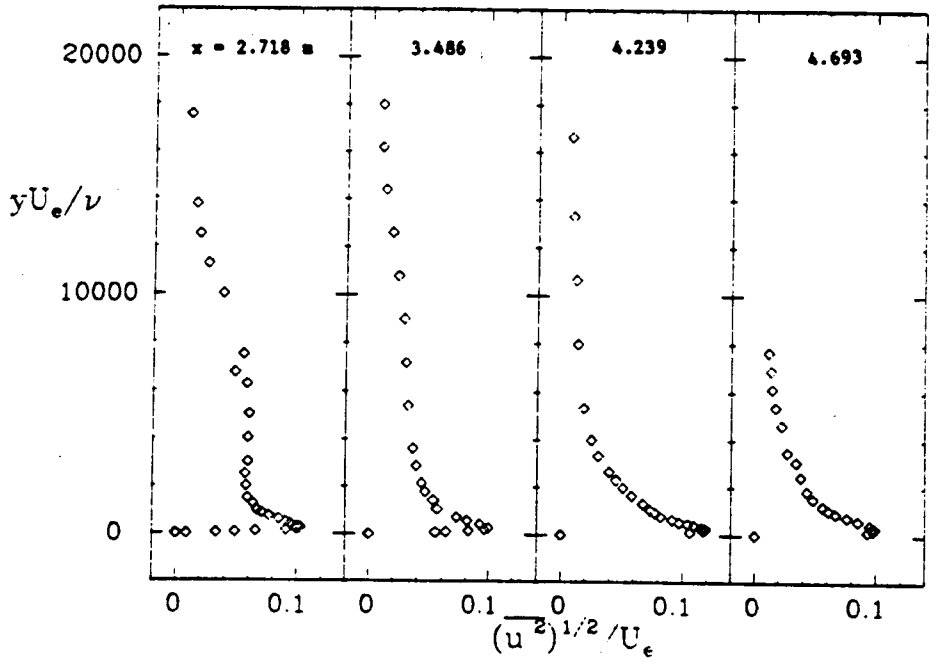

Figure 16. Boundary layer turbulence intensity profiles for relaminarizing flow [10]. Increasing values of x denote downstream progress towards relaminarization.

The results in Figures 14 and 15 raise the question of a class of boundary layers which lie between the fully laminar and fully turbulent states. In the case of the external turbulence flows, the terms "pseudo-laminar" and "pseudo-turbulent" have been used. In consideration of where they lie in terms of shape parameter values, the term "transitional" may be more appropriate. The implication of the data in the figures is that a "transitional" shape factor correlation curve may exist which connects laminar and turbulent flows. This concept will be investigated in the effort to develop a practical boundary layer prediction method for the slipstream case.

SUMMARY

The laminar boundary layer within a propeller slipstream is affected by the viscous wake from the propeller blade. The wake forms

a helical sheet which is split by the wing and passes over the upper and lower surfaces. Across a propeller blade wake passage cycle, the boundary layer at a point on the airfoil surface goes through the distinct phases of turbulent, reverse-transitional and laminar behavior consistent with a cyclic variation in external flow turbulence. The turbulent phase is characteristic of boundary layer flow with external turbulence, and exhibits velocity profiles which lie in a transitional region between fully laminar and fully turbulent flow. The cyclic external turbulence may also influence the turbulent boundary layer in such a way as to cause periodic relaminarization as has been observed in flight and in the wind tunnel.

ACKNOWLEDGEMENT

This work is supported by NASA Langley Research Center
Grant No. NAG 1-344.

REFERENCES

1. Young, A.D. and Morris, D.E., "Note on Flight Tests on the Effect of Slipstream on Boundary Layer Flow," R&M No. 1957, Brit. A.R.C., 1939.

2. Young, A.D. and Morris, D.E., "Further Note on Flight Tests on the Effect of Slipstream on Boundary-Layer Flow," RAE Rep. No. B.A. 1404b, 1939.

3. Hood, M.J. and Gaydos, M.E., "Effects of Propellers and Vibration on the Extent of Laminar Flow on the NACA 27-212 Airfoil," NACA ACR (WR L-784), 1939.

4. Zalovcik, J.A., "Flight Investigation of the Boundary Layer and Profile Drag Characteristics of Smooth Wing Sections on a P-47D Airplane," NACA WR L-86, 1945.

5. Zalovcik, J.A., and Skoog, R.B., "Flight Investigation of Boundary Layer Transition and Profile Drag of an Experimental Low-Drag Wing Installed on a Fighter-Type Airplane," NACA WR L-94, 1945.

6. Holmes, B.J., Obara, C.J., and Yip, L.P., "Natural Laminar Flow Experiments on Modern Airplane Surfaces," NASA TP 2256, 1984.

7. Holmes, B.J., Obara, C.J., Gregorek, G.M., Hoffman, M.J., and Freuhler, R.J., "Flight Investigation of Natural Laminar Flow on the Bellanca Skyrocket II," SAE Paper 830717, 1983.

8. Sparks, S.P. and Miley, S.J., "Development of a Propeller Afterbody Analysis with Contracting Slipstream," SAE Technical Paper Series 830743, April 1983.

9. Dyban, Ye.P., Epik, E.Ya., and Surpun, T.T., "Characteristics of the Laminar Boundary Layer in the Presence of Elevated Free-Stream Turbulence," Fluid Mechanics - Soviet Research, Vol. 5, No. 4, July-August 1976, pp. 30-36.

10. Kline, S.J., Cantwell, B.J. and Lilley, G.M., ed. "The 1980-81 AFSOR-HTTM-Stanford Conference on Complex Turbulent Flows: Comparison of Computation and Experiment," Thermosciences Division, Mechanical Engineering Department, Stanford University, 1981.

11. Eppler, R. and Somers, D.M., "A Computer Program for the Design and Analysis of Low-Speed Airfoils," NASA TM 80210, 1980.